

Cosmogenic nuclide and solute flux data from central Cuban rivers emphasize the importance of both physical and chemical mass loss from tropical landscapes.

Mae Kate Campbell^{1,2}, Paul R. Bierman^{2,3}, Amanda H. Schmidt⁴, Rita Sibello Hernández⁵, Alejandro García-Moya⁵, Lee B. Corbett³, Alan J. Hidy⁶, Héctor Cartas Águila⁵, Aniel Guillén Arruebarrena⁵, Greg Balco⁷, David Dethier⁸, Marc Caffee⁹

¹Department of Geology, University of Vermont, Burlington, VT 05405, USA

²Gund Institute for Environment, University of Vermont, Burlington, VT 05405

³Rubenstein School of the Environment and Natural Resources, the University of Vermont, Burlington, VT 05405, USA

⁴Department of Geosciences, Oberlin College, Oberlin, OH 44074, USA

⁵Centro de Estudios Ambientales de Cienfuegos, Departamento de Estudio de la Contaminación Ambiental. AP 5, 59350, Ciudad Nuclear, Cienfuegos, Cuba

⁶Atmospheric, Earth, and Energy Division, Lawrence Livermore National Laboratory, Livermore, CA 94550, USA

⁷Berkeley Geochronology Center, Berkeley, CA 94709, USA

⁸Department of Geosciences, Williams College, Williamstown, MA 01267, USA

⁹Department of Physics and Astronomy and Department of Earth, Atmospheric, and Planetary Sciences, Purdue University, West Lafayette, IN 47907, USA

Correspondence to: Amanda H. Schmidt (aschmidt@oberlin.edu)

Style Definition: Normal: Font: 12 pt, (Asian) Chinese (China), (Other) English (US), Left, Line spacing: single

Style Definition: Heading 1: Font: 10 pt, English (UK), Justified

Style Definition: Heading 2: Font: 10 pt, English (UK), Justified

Style Definition: Heading 3: Font: 10 pt, English (UK), Justified

Style Definition: Heading 4: Font: 10 pt, English (UK), Justified, Line spacing: 1.5 lines

Style Definition: Betreff: Font: 10 pt, English (UK), Justified, Line spacing: 1.5 lines

Style Definition ... [10]

Style Definition ... [9]

Style Definition: Kontakt: English (UK), Justified

Style Definition ... [8]

Style Definition ... [7]

Style Definition: MS title: English (UK), Justified

Style Definition ... [6]

Style Definition ... [5]

Style Definition: Balloon Text: English (UK), Justified

Style Definition ... [4]

Style Definition: Caption: English (UK), Justified

Style Definition: Footer: Font: 10 pt, English (UK), Justified

Style Definition ... [3]

Style Definition: Authors: English (UK), Justified

Style Definition ... [2]

Style Definition: EndNote Bibliography: Justified

Style Definition ... [1]

Formatted: Font: 12 pt

Formatted ... [11]

Deleted: Cuba

Formatted: Font: 12 pt

Deleted: denudation in highly weathered

Formatted: Font: 12 pt

Formatted: Font: 12 pt

Formatted ... [12]

Deleted: Corbett¹

Deleted: Geology

Formatted: Font: 12 pt

Abstract

We use 25 new measurements of *in situ* produced cosmogenic ^{26}Al and ^{10}Be in river sand, paired with estimates of dissolved load flux in river water, to characterize the processes and pace of landscape change in central Cuba. Long-term erosion rates inferred from ^{10}Be concentrations in quartz extracted from central Cuban river sand range from 3.4-189 $\text{Mg km}^{-2} \text{y}^{-1}$ (mean = 59, median = 45). Dissolved loads (10-176 $\text{Mg km}^{-2} \text{y}^{-1}$; mean = 92, median = 97), calculated from stream solute concentrations and modelled runoff, exceed measured cosmogenic ^{10}Be -derived erosion rates in 18 of 23 basins. This disparity mandates that landscape-scale, in this environment, mass loss is not fully represented by the cosmogenic nuclide measurements.

The $^{26}\text{Al}/^{10}\text{Be}$ ratios are lower than expected for steady-state exposure or erosion in 16 of 24 samples. Depressed $^{26}\text{Al}/^{10}\text{Be}$ ratios occur in many of the basins that have the greatest disparity between dissolved loads (high) and erosion rates inferred from cosmogenic nuclide concentrations (low). Depressed $^{26}\text{Al}/^{10}\text{Be}$ ratios are consistent with the presence of a deep, mixed, regolith layer providing extended storage times on slopes and/or burial and extended storage during fluvial transport. River water chemical analyses indicates many basins with lower $^{26}\text{Al}/^{10}\text{Be}$ ratios and high ^{10}Be ratios are underlain at least in part by evaporitic rocks that rapidly dissolve.

Our data show that when assessing mass loss in humid tropical landscapes, accounting for the contribution of rock dissolution at depth is particularly important. In such warm, wet climates, mineral dissolution can occur many meters below the surface, beyond the penetration depth of most cosmic rays, and thus the production of most cosmogenic nuclides. Our data suggest the importance of estimating solute fluxes and measuring paired cosmogenic nuclides to understand better the processes and rates of mass transfer at a basin-scale.

1 Introduction

Cosmogenic nuclide concentrations of river sand have been used to quantify rates of landscape change (often termed erosion rates) since the 1990s (Brown et al., 1995; Granger et al., 1996; Bierman and Steig, 1996; Portenga and Bierman, 2011; Codilean et al., 2018). Accurately establishing long-term

- Deleted: ...e use 25 newconsider...measurements of bot (... [13])
- Formatted (... [14])
- Deleted: 7-182 tons
- Formatted (... [15])
- Deleted: yr
- Formatted (... [16])
- Deleted: 62
- Formatted (... [17])
- Deleted: 57). Rock dissolution rates (24-154 tons
- Formatted (... [18])
- Deleted: yr
- Formatted (... [19])
- Deleted: 84
- Formatted (... [20])
- Deleted: 78) inferred
- Formatted (... [21])
- Deleted: loads
- Formatted (... [22])
- Deleted: nuclide
- Formatted (... [23])
- Deleted: sediment generation
- Formatted (... [24])
- Deleted: 15
- Formatted (... [25])
- Deleted: 22
- Formatted (... [26])
- Deleted: , indicating significant ...andscape-scale, in this (... [27])
- Formatted (... [28])
- Deleted: that of surface production are consistent with the (... [29])
- Formatted (... [30])
- Deleted: disagreement
- Formatted (... [31])
- Deleted: rock dissolution rates
- Formatted (... [32])
- Deleted: sediment generation
- Formatted (... [33])
- Formatted (... [34])
- Formatted (... [35])
- Formatted (... [36])
- Deleted: mineral
- Formatted (... [37])
- Deleted: in calculations of total denudation
- Formatted (... [38])
- Deleted: in the humid tropics, where dissolved load fluxe (... [39])
- Formatted (... [40])
- Deleted: Relying on cosmogenic nuclide data or stream sc (... [41])
- Formatted (... [42])
- Formatted (... [43])
- Formatted (... [44])
- Deleted: This study presents measurements of cosmogeni (... [45])

160 rates of change provides an important context for understanding the effects of human activity on erosion (Reusser et al., 2015; Nearing et al., 2017), and for other common applications of cosmogenic nuclides at the basin-scale, such as quantifying the effect of tectonics (Scherler et al., 2014), climate (Marshall et al., 2017), and baselevel change (Reinhardt et al., 2007) on rates of landscape change over time.

¹⁰Be-derived rates of landscape change at a drainage-basin scale are often implicitly assumed to reflect both physical and chemical mass loss, the sum of which is termed denudation (Regard et al., 2016). However, this assumption is only valid if all mass loss from the landscape occurs within the uppermost meter or two of Earth's surface, the penetration depth of the cosmic-ray neutrons responsible for producing most cosmogenic nuclides via spallation reactions (Bierman and Steig, 1996). Deeper mass loss by rock dissolution remains largely undetected by cosmogenic nuclide analysis. Failure to account for rock dissolution at depth and the export of mass as dissolved load below the spallation-dominated nuclide production zone (~2 m) may bias cosmogenic nuclide-derived estimates of denudation (Small et al., 1999; Riebe et al., 2001a; Dixon et al., 2009a) on the low side. Incorrectly determined erosion rates can derail attempts to understand landscape evolution, soil production, and climate interaction with surface processes (Riebe et al., 2003).

175 Rock dissolution at depth is a major process in areas with significant groundwater-rock interactions; connecting denudation rates to landscape change requires consideration of this process. This includes any landscape where the physical removal of mass is slow, allowing for prolonged water-rock interactions, such as low-relief landscapes (Ollier, 1988). Some landscape characteristics facilitate or are the result of extensive water-rock interaction; thick saprolite (Dixon et al., 2009a), extensively jointed/fractured bedrock (Ollier, 1988), and readily soluble rocks, including carbonate (Pope, 2013), and evaporite deposits. Conditions in the humid tropics favor prolonged and extensive water rock-interaction and include the absence of recent glaciation (Modenesi-Gauttieri et al., 2011), the presence of active groundwater flow systems year-round (Ollier, 1988), and large amounts of precipitation.

185 Rock dissolution rates in the tropics can be among the highest globally (Pope, 2013); yet, global compilations of cosmogenic nuclide data from river sand suggest rates of landscape change in the tropics are slower than in most other climate zones (Portenga and Bierman, 2011). This dichotomy is consistent with cosmogenic rates significantly underestimating landscape denudation in areas where

Formatted: Don't adjust right indent when grid is defined, Line spacing: 1.5 lines, Don't snap to grid

Deleted: . Cosmogenic nuclides are commonly used to infer combined rates of physical erosion and rock dissolution (Regard et al., 2016), also referred to as chemical weathering, under the assumption that both occur primarily within the uppermost meter or two of Earth's surface, the penetration depth of the cosmic ray neutrons responsible for producing most cosmogenic nuclides via spallation reactions (Bierman and Steig, 1996). Such rates are often assumed to represent total landscape denudation, but failure to account for rock dissolution at depth and the export of mass as dissolved load below the spallation-dominated production zone (below ~2 m) can result in a low bias for cosmogenic nuclide-derived erosion rate estimates (Small et al., 1999; Riebe et al., 2001a; Dixon et al., 2009a). Measuring both physical erosion and rock dissolution is essential for understanding landscape evolution, soil production, and climate regulation (Riebe et al., 2003). Accurately establishing long-term denudation rates provides important context for understanding the effects of human activity on erosion (Reusser et al., 2015; Nearing et al., 2017), and for other common applications of cosmogenic nuclides at the basin-scale, such as quantifying the effect of tectonics (Scherler et al., 2014), climate (Marshall et al., 2017), and baselevel change (Reinhardt et al., 2007) on rates of landscape change over time.

Deleted: Accounting for rock

Deleted: particularly important for interpreting rates of landscape change ...

Deleted: the potential for

Deleted: at depth.

Deleted: (Ollier, 1988)

Deleted: Landscape features that

Deleted: , such as

Deleted: (Ollier, 1988), or

Deleted: such as karst systems (Pope, 2013)

Deleted: can also contribute to significant rock dissolution at depth. Such landscapes can develop in any climate; however (... [46])

Deleted: are often favorable for

Deleted: . The

Deleted: (Modenesi-Gauttieri et al., 2011),

Deleted: (Ollier, 1988)

Deleted: create ideal conditions for rock dissolution at depth.

Deleted: are

Deleted: (Pope, 2013)

Deleted: sediment generation

Deleted: (Portenga and Bierman, 2011),

Deleted: the potential for

Deleted: nuclide-derived

Deleted: of landscape change to

Deleted: underestimate total

deep rock dissolution is ubiquitous. Only a few studies focused in the tropics compare nuclide-derived rates to measurements of dissolved load flux in streams (e.g. Salgado et al., 2006; Hinderer et al., 2013; Regard et al., 2016). As the use of cosmogenic nuclides to measure rates of landscape change in the

Deleted: erosion

tropics expands (e.g. Cherem et al., 2012; Barreto et al., 2013; Derrieux et al., 2014; Mandal et al., 2015; Sosa Gonzalez et al., 2016a; Jonell et al., 2017), considering the potential influence of rock dissolution at depths below the production of most cosmogenic nuclides becomes more important. Here, we present measurements of *in situ* ²⁶Al and ¹⁰Be in riverine quartz, along with estimates of dissolved loads, in humid, tropical central Cuba (Bierman et al., 2020). With these data, we explore

Deleted: depth and thus not captured in

Deleted: nuclide-derived erosion rates will lead to

Deleted: accurate estimates of total denudation. Basin-wide rock dissolution rates can be quantified by measuring river water chemistry and flow over time (Dunne, 1978); however, only a few studies focused in the tropics compare cosmogenic nuclide-derived rates of sediment generation to measurements of dissolved load flux in streams (e.g. Salgado et al., 2006; Hinderer et al., 2013; Regard et al., 2016).

Deleted: explore the relationships between surface denudation and rock dissolution at depth in a tropical landscape where mass is being lost by multiple processes. We measured

Deleted: and stream water

Deleted: to

Deleted: to

Deleted: Throughout this paper, we refer to rates of landscape mass loss calculated from ²⁶Al and ¹⁰Be as sediment generation rates, and rates of landscape mass loss inferred from measurements of stream water dissolved loads as rates of rock dissolution—all in units of mass per unit area over time.

2 Background

Formatted: Font: 12 pt

Terminology referring to mass loss from watersheds has been applied ambiguously in the past and can be confusing. Here, we refer to the tempo of landscape mass loss calculated from ²⁶Al and ¹⁰Be concentrations as erosion rates; these rates include all processes (physical and chemical) removing mass within ~2 m of Earth's surface. We refer to rates of landscape mass loss inferred from measurements of stream water chemistry, convolved with estimates of annual run-off volumes, as rock dissolution rates. We use the term denudation to refer to total mass loss from sampled catchments. All of these rates are expressed in terms of mass per time per area (Mg km⁻² y⁻¹), which can be converted to depth over time by assuming a rock density.

2.1 Quantifying basin mass loss with cosmogenic nuclides: approaches and limitations

Landscape-scale denudation occurs through both physical removal of mass (erosion) and chemical dissolution of minerals in rocks. Sediment, produced from eroding bedrock, travels downslope towards base level, whereas rock dissolution moves mass in solution from the landscape to rivers, and then to the ocean. Measurement of cosmogenic nuclides in river sediment can be used to infer the spatially averaged erosion rate of a drainage basin (Brown et al., 1995; Granger et al., 1996; Bierman and Steig, 1996). In a basin that is steadily eroding, the concentration of cosmogenic nuclides in a sediment sample reflects the rate at which overlying mass at and near the surface was removed as the material was exhumed, through both physical mass loss and rock dissolution (Lal, 1991). Cosmogenic erosion rates are equivalent to denudation rates if, and only if, rock dissolution only occurs within a meter or two of the surface—the depth of penetration for neutrons which produce most cosmogenic nuclides. If rock dissolution occurs below the neutron penetration depth, erosion rates calculated from measured nuclide concentrations will underestimate denudation.

Measuring multiple cosmogenic nuclides with different half lives in the same sample can provide more information on the near-surface history of surface materials, such as soil mixing depth and residence time (Lal and Chen, 2005), as well as sediment storage within the watershed (Granger and Muzikar, 2001). The production ratio of $^{26}\text{Al}/^{10}\text{Be}$ at the surface at mid- and low-latitudes is constrained by measurements and nuclear physics (Nishiizumi et al., 1989; Balco et al., 2008). If sediment that has accumulated cosmogenic nuclides is buried such that production is diminished over $> 10^5$ y, the production ratio decreases because ^{26}Al decays more rapidly than ^{10}Be . Vertical soil mixing intermittently buries sediment grains, suppressing the $^{26}\text{Al}/^{10}\text{Be}$ ratio in sediment shed from the landscape surface (Makhubela et al., 2019).

Paired cosmogenic isotope concentrations are visualized using a two-isotope diagram; the y-axis is the $^{26}\text{Al}/^{10}\text{Be}$ ratio and the x-axis is the concentration of ^{10}Be with normalization based on the production rate of nuclides at the sample site (Klein et al., 1986; Granger, 2006). Sediment samples that have experienced constant exposure with no erosion, or constant exposure under steady-state erosion, will plot within an enclosed region along the top of the diagram; samples that have experienced more complex exposure histories, including burial during or after cosmic-ray exposure, will plot below this

Formatted: Font: 12 pt

Deleted: denudation

Formatted: Font: 12 pt

Formatted: Don't adjust right indent when grid is defined, Line spacing: 1.5 lines, Don't snap to grid

Deleted: by

Deleted: sediment generation

Deleted: , but does not provide insight about processes—such as rock dissolution—occurring at depth. Assuming a density of the source rock, one can calculate equivalent rates of landscape lowering over time.

Deleted: erosion

Deleted: (Lal, 1991)

Deleted: Measuring multiple cosmogenic nuclides with different half lives in the same sample can provide more information on the exposure history of surface materials, such as soil mixing and residence time (Lal and Chen, 2005), as well as sediment storage within the watershed (Granger and Muzikar, 2001). The production ratio of $^{26}\text{Al}/^{10}\text{Be}$ at the surface at mid- and low-latitudes is ~ 6.75

Formatted: Don't adjust right indent when grid is defined, Line spacing: 1.5 lines, Don't snap to grid

region. Such complex histories could include development of a vertically mixed surface layer (Bierman, 1999; Lal and Chen, 2005) as well as extended burial during transport down slopes and in and along rivers.

Using measurements of cosmogenic nuclides to determine basin-averaged denudation rates requires the assumptions that mass loss from the basin is in steady-state, that the mineral used for cosmogenic nuclide measurements is uniformly distributed throughout the watershed, and that denudation occurs within the penetration depth of most cosmic rays, the upper several meters of Earth's surface (Bierman and Steig, 1996). The grain size fraction selected for cosmogenic nuclide analysis must also be representative of the grain size distribution of sediment being produced on slopes (Lukens et al., 2016) although in many landscapes cosmogenic nuclide concentrations do not vary by sediment grainsize.

Erosion rates calculated from cosmogenic nuclides can be inaccurate if these assumptions are violated. Rock dissolution can leave sediment enriched in resistant mineral phases, such as zircon, titanite, and quartz—the mineral in which ^{26}Al and ^{10}Be are most commonly measured (Riebe and Granger, 2013). Such enrichment produces underestimates of long-term denudation rates unless accounted for, because the enriched mineral will have a longer residence time relative to the surrounding regolith (Riebe et al., 2001a; Ferrier and Kirchner, 2008). Calculations of denudation rates from cosmogenic nuclide concentrations also rely on the assumption that mass loss is occurring primarily through surface lowering; however, some rock dissolution and, thus, some transfer of mass from rock to groundwater solutions occurs below the depth of most cosmogenic nuclide production (Fig. 1; Small et al., 1999; Dixon et al., 2009a; Riebe and Granger, 2013). In areas with significant rock dissolution at depth, denudation rates inferred from cosmogenic nuclides underestimate denudation because some mass loss occurs below the depth of most nuclide production.

2.2 Chemical weathering corrections to cosmogenically-determined mass loss rates

Although the importance of accounting for loss of mass by chemical weathering (rock dissolution) when calculating cosmogenic erosion rates has been recognized (Small et al., 1999; Riebe et al., 2001a; Dixon et al., 2009a; Riebe and Granger, 2013), few studies incorporate rock dissolution

Deleted: . If sediment that has accumulated cosmogenic nuclides is buried such that production is negligible, this ratio decreases because ^{26}Al decays more rapidly than ^{10}Be . Similarly, vertical mixing within a soil column has the effect of increasing the near-surface residence time of sediment grains, suppressing the $^{26}\text{Al}/^{10}\text{Be}$ ratio in sediment shed from the landscape surface during erosion (Makhubela et al., 2019). Isotope concentrations are commonly examined using a 2-isotope diagram, in which the y-axis is the $^{26}\text{Al}/^{10}\text{Be}$ ratio and the x-axis is the concentration of ^{10}Be (Klein et al., 1986; Granger, 2006). Sediment samples that have experienced constant exposure with no erosion, or constant exposure under steady-state erosion conditions, will plot within the simple exposure region along the top of the diagram; samples that have experienced more complex exposure histories, including burial during or after cosmic-ray exposure, will plot below this region. Such complex histories could include development of a vertically mixed surface layer (Bierman, 1999; Lal and Chen, 2005).

Deleted: long-term total

Deleted: erosion of

Deleted: (Bierman and Steig, 1996).

Deleted: .

Deleted: Denudation

Deleted: may not represent total landscape denudation rates

Deleted: methodological

Deleted: (Riebe and Granger, 2013).

Deleted: (Riebe et al., 2001a; Ferrier and Kirchner, 2008)

Deleted: total

Deleted: 2.2 Subsection (as Heading 2)

Formatted: Font: 12 pt

Deleted: denudation

information or apply correction factors to cosmogenic nuclide-derived rates. In the tropics, some studies compare export rates from dissolved loads in streams to cosmogenically-derived erosion rates, but those studies have considered these two metrics of landscape change separately (Von Blackenburg et al., 2004; Salgado et al., 2006; Hinderer et al., 2013). Other studies use the measurement of insoluble elements in bedrock, saprolite, and soil to quantify quartz enrichment through the weathering process and calculate correction factors that account for the influence of rock dissolution at and near the surface (Small et al., 1999; Riebe et al., 2001a), at depth (Dixon et al., 2009b), or both (Riebe and Granger, 2013).

Of studies that do correct for the influence of chemical weathering when calculating cosmogenic nuclide-derived rates of erosion, Riebe and Granger (2013)'s chemical erosion factor (CEF) method, or earlier quartz enrichment factor method (Riebe et al., 2001a), are often used (Regard et al., 2016). Calculating a CEF requires measurements of soil thickness and density, as well as determining the concentration of the mineral used in cosmogenic nuclide measurements (commonly quartz) and an insoluble element (commonly Zr) in numerous samples of soil, saprolite, and unweathered bedrock. The method is underpinned by the assumption that chemical mass loss is occurring exclusively in well-mixed regolith and deep saprolite (Riebe and Granger, 2013). Erosion rates calculated from cosmogenic nuclide measurements can be multiplied by the CEF to correct for the effects of chemical mass loss (Riebe and Granger, 2013). Chemical erosion factors reported in tropical environments include a CEF of 1.79 in Puerto Rico (Riebe and Granger, 2013) and 3.2 in Cameroon (Regard et al., 2016), demonstrating how significantly cosmogenic nuclide-derived estimates of erosion can underestimate total denudation rates by not accounting for the effects of deep rock dissolution.

3 Study area

Cuba is the largest Caribbean island (~110,000 km²) and is situated along the boundary between the Caribbean and North American plates. Reflecting this complex tectonic setting, Cuban geology is varied and includes silicate, carbonate, and evaporite rocks (Pardo, 2009). Lithologies include marine deposits, accreted volcanic terrains, passive-margin sediments, and obducted ophiolite, all

Deleted: have compared

Deleted: catchment-averaged sediment generation

Deleted: from cosmogenic nuclide measurements, but

Deleted: More broadly, other

Deleted: (Small et al., 1999; Riebe et al., 2001a)

Deleted: (Dixon et al., 2009b)

Deleted: (Riebe and Granger, 2013)

Deleted: Of studies that do correct for the influence of chemical weathering when calculating cosmogenic nuclide-derived denudation rates, Riebe and Granger (2013)'s chemical erosion factor (CEF) method, or earlier quartz enrichment factor method (Riebe et al., 2001a), are often used (Regard et al., 2016). Calculating a CEF requires measurements of soil thickness and density, and determining the concentration of the mineral used in cosmogenic nuclide measurements (commonly quartz) and an insoluble element (commonly Zr) in numerous samples of soil, saprolite, and unweathered bedrock; the method is underpinned by the assumption that chemical erosion is occurring exclusively in well-mixed soils and deep saprolite (Riebe and Granger, 2013). Denudation rates calculated from cosmogenic nuclide measurements can be multiplied by the CEF to correct for the effects of deep and near surface chemical erosion (Riebe and Granger, 2013). Chemical erosion factors reported in tropical environments include a CEF of 1.79 in Puerto Rico (Riebe and Granger, 2013) and 3.2 in Cameroon (Regard et al., 2016), demonstrating how significantly cosmogenic nuclide-derived estimates of denudation can underestimate total denudation rates by not accounting for the effects of rock dissolution...

Formatted: Font: 12 pt

Deleted: (Pardo, 2009)

Deleted: Basement lithologies

unconformably overlain by slightly-deformed autochthonous coarse elastic sediment and limestone (Iturralde-Vinent et al., 2016).

Deleted: clastics

Deleted: (Iturralde-Vinent et al., 2016)

440 The Cuban landscape features a mountainous spine (600-1970 m) descending into low relief coastal plains, except along portions of the south coast where mountains meet the sea. This drainage divide parallels Cuba's east-west orientation, creating rivers that travel relatively short distances from headwaters to base level (Galford et al., 2018). Cuba's climate is tropical wet and dry, with a mean annual temperature of 24.5 °C and average annual precipitation of 1335 mm y⁻¹. The climate is highly seasonal; ~80% of this precipitation is delivered during the wet season from May-October (Llacer, 2012).

Formatted: Don't adjust right indent when grid is defined, Line spacing: 1.5 lines, Don't snap to grid

Deleted: (Galford et al., 2018).

445 Centuries of agriculture have heavily altered the Cuban landscape (Whitbeck, 1922). Prior knowledge of mass loss at the basin scale is limited to measurements of suspended sediment discharge for short periods between 1964 and 1983 for 32 Cuban rivers (Pérez Zorrilla and Ya Karasik, 1989), and 450 measurements of dissolved loads in five limestone basins with karst (Pulina and Fagundo, 1992). In central Cuba, underlying basin rock type is the primary control on surface water geochemistry (Betancourt et al., 2012), a finding supported by geochemical analyses of river waters from the same basins sampled in this study (Bierman et al., 2020). Dissolved load fluxes carried by Cuban rivers (Bierman et al., 2020), and rock dissolution rates inferred from these fluxes, are consistent with rates 455 reported for other Caribbean islands [Dominica, Guadeloupe, and Martinique from Rad et al. (2013), and Puerto Rico from White and Blum (1995)], and high compared to global data compiled by Larsen et al. (2014a).

Deleted: /yr;

Deleted: (Llacer, 2012)

Deleted: The Cuban landscape has been

Deleted: by agriculture for centuries (Whitbeck, 1922).

Deleted: (Pérez Zorrilla and Ya Karasik, 1989)

Formatted: Font: 12 pt

Deleted: (Betancourt et al., 2012)

Deleted: (Bierman et al., 2020)

Deleted: (Bierman et al., 2020)

Deleted: Rad et al. (2013)

Deleted: White and Blum (1995)

Deleted: Larsen et al. (2014)

Formatted: Font: 12 pt

Moved (insertion) [1]

Deleted: Bierman et al. (2020) for photos/descriptions of select field sites). Three sample sites are near previously-gauged hydrologic stations with discharge and suspended sediment records spanning 9-15 years (Pérez Zorrilla and Ya Karasik, 1989). We extracted drainage basins and then calculated basin slopes and effective elevations (Portenga and Bierman, 2011) using the ASTER Global Digital Elevation Model (Lpdaac), determined underlying basin rock types from the USGS Caribbean layer (French and Schenk, 2004)

4 Methods

4.1 Field methods

460 We collected detrital sediment (n = 26) from the beds of active river channels in central Cuba, representing a variety of basin sizes, average slopes, and lithologies (Fig. 2; Supplement T1-2). Channel morphologies varied, but most streams were incised, and many had exposed bedrock (see Bierman et al. (2020) for photos/descriptions of select field sites). At each site we collected samples for water

Moved down [2]: , and utilized precipitation data from the WorldClim dataset (Hijmans et al., 2005) to estimate basin-specific mean annual precipitation (MAP).

Moved up [1]: We collected detrital sediment (n = 26) from the beds of active river channels in central Cuba, representing a variety of basin sizes, average slopes, and lithologies (Fig. 2; Supplement T1-2). Channel morphologies varied, but most streams were incised, and many had exposed bedrock (see

495 [chemistry analysis and measured channel parameters, including width, depth, and discharge at time of sampling.](#)

4.2 Lab methods

Formatted: Font: 12 pt

500 We prepared samples for cosmogenic analysis and extracted beryllium and aluminum following the methodology of Corbett et al. (2016). We sieved bulk sediment samples in the lab and used the 250-850 μm grain size fraction for all samples, except for CU-120, which also includes finer material (63-250 μm) due to low quartz content. [Sediment samples were chemically etched to purify quartz and remove meteoric \$^{10}\text{Be}\$ \(Kohl and Nishiizumi, 1992\).](#) Twenty-four samples yielded sufficient quartz for analysis. We measured quartz yields for all [but one sample \(CU-120\)](#) by recording the mass of sediment before and after dilute acid etching ([Supporting Fig. 1](#)).

Deleted: Sediment samples were chemically etched to purify quartz and remove meteoric ^{10}Be (Kohl and Nishiizumi, 1992)

Deleted: 24

Deleted: (including all 3 gauging station samples)

Deleted: samples

Deleted: .

Formatted: Font color: Text 1

Formatted: Don't adjust right indent when grid is defined, Line spacing: 1.5 lines, Don't snap to grid

Deleted: 40

Formatted: Font color: Text 1

505 We extracted ^{26}Al and ^{10}Be at the National Science Foundation/ University of Vermont Community Cosmogenic Facility, using [~5-43 g](#) of quartz per sample (mean = 24 g). We added ~250 μg of Be to each sample using two different in-house made carriers (Supplement T5); the first batch used a low-ratio carrier made from beryl, while subsequent batches used a dilution of low-ratio commercial SPEX carrier. We added Al to samples with insufficient total Al using a commercial SPEX ICP standard in order to reach a total Al mass of ~1500 μg (Supplement T6). Samples were processed in batches of 12, each of which included at least one blank, and two batches included one quality control standard each ([Corbett et al., 2019](#)).

Deleted: (Corbett et al., 2019)

Deleted: ^{27}Al /

Deleted: Spectrometer

Deleted: ^{27}Al /

Deleted: (Nishiizumi, 2004)

Deleted: Laboratory

Formatted: Font color: Text 1

Deleted: two

Formatted: Font color: Text 1

Deleted: in-house made

Formatted: Font color: Text 1

Deleted: 3

Formatted: Font color: Text 1

Deleted: 14

Formatted: Font color: Text 1

Deleted: 19

Formatted: Font color: Text 1

515 $^{10}\text{Be}/^9\text{Be}$ and $^{26}\text{Al}/^{27}\text{Al}$ measurements ($n = 26$, including 2 duplicates), were made by Accelerator Mass Spectrometry (AMS) at the Purdue Rare Isotope Measurement Laboratory (PRIME). ^{10}Be ratios were normalized against standard 07KNSTD3110 with an assumed ratio of 2850×10^{-15} (Nishiizumi et al., 2007) and $^{26}\text{Al}/^{27}\text{Al}$ measurements were normalized against standard KNSTD with an assumed ratio of 1818×10^{-15} (Nishiizumi, 2004). [Full laboratory replicate sample preparations and](#) measurements of ^{26}Al and ^{10}Be agree to within $< 2\%$ (Supplement T7; $n=2$). We corrected Be measurements by carrier type, since samples were prepared using [different carriers; we use the average](#) of two process blanks ($1.91 \pm 1.01 \times 10^{-15}$; 1SD) to correct 10 samples, and the average of [four](#) process blanks ($4.02 \pm 1.00 \times 10^{-15}$; 1SD) for the remaining samples (Supplement T3). We corrected Al

540 measurements using the average of 4 process blanks ($4.97 \pm 2.94 \times 10^{-15}$; Supplement T4). We subtracted blank ratios from sample ratios and propagated uncertainties in quadrature.

Deleted: a single

Deleted: blank (1.92 ± 1.36)

Formatted: Font color: Text 1

Formatted: Font color: Text 1

Formatted: Font: 12 pt

4.3 Analytical methods

545 We extracted drainage basins and then calculated basin slopes and effective elevations (Portenga and Bierman, 2011) using the ASTER Global Digital Elevation Model (Lp Daac), determined underlying basin rock types from the USGS Caribbean layer (French and Schenk, 2004), and utilized precipitation data from the WorldClim dataset (Hijmans et al., 2005) to estimate basin-specific mean annual precipitation (MAP).

Deleted: We calculated erosion rates using version 3 of the online erosion rate calculator originally described by Balco et al. (2008) and subsequently updated [wrapper: 3.0, erates: 3.0, muons: 3.1, validate: validate_v2_input.m - 3.0 consts: 2020-08-26] using the effective elevation (Portenga and Bierman, 2011) calculated for the basin upstream of the sample collection point, a sample thickness of 0 cm, a density of 2.6 g cm^{-3} , and assuming no topographic shielding across this low-relief landscape. We report erosion rates using the Lal-Stone (St) (Lal, 1991; Stone, 2000) production scaling scheme.

Moved (insertion) [2]

550 We calculated erosion rates using version 3 of the online erosion rate calculator originally described by Balco et al. (2008) and subsequently updated (wrapper: 3.0, erates: 3.0, muons: 3.1, validate: validate_v2_input.m - 3.0 consts: 2020-08-26) using the effective elevation (Portenga and Bierman, 2011) calculated for the basin upstream of the sample collection point, a sample thickness of 0 cm, a rock density of 2.6 g cm^{-3} , and assuming no topographic shielding across this low-relief landscape. We report erosion rates using the Stone/Lal production scaling scheme.

Formatted: Don't adjust right indent when grid is defined, Line spacing: 1.5 lines, Don't snap to grid

555 For samples with the highest ^{10}Be concentrations ($n=4$), we also measured the concentration of cosmogenic ^{21}Ne in quartz to further characterize exposure history (Supplement T10). Neon isotope measurements were made at the Berkeley Geochronology Center on aliquots of the same purified quartz samples used for $^{26}\text{Al}/^{10}\text{Be}$ analysis. They were done by vacuum degassing and noble gas mass spectrometry using the method described in Balter-Kennedy et al. (2020) and Balco and Shuster (2009).

Deleted: Finally, for four samples with the highest ^{10}Be concentrations, we also measured concentrations of cosmogenic ^{21}Ne in quartz as an attempt to further distinguish simple and complex exposure histories (Supplement T10). Neon isotope measurements were made at the Berkeley Geochronology Center on aliquots of the same purified quartz samples used for $^{26}\text{Al}/^{10}\text{Be}$ analysis. They were done by vacuum degassing and noble gas mass spectrometry using the method described in Balter-Kennedy et al. (2020) and Balco and Shuster (2009).

560 We used measurements of dissolved loads in stream water (Bierman et al., 2020) and modelled annual flows from GLOH2O (Beck et al., 2015; Beck et al., 2017) to calculate rock dissolution rates for the 25 basins where we were able to collect water samples. To account for the wide range of lithologies in our upstream watersheds, including some with evaporites, we modified the approach used by Erlanger et al. (2021) (Supporting Fig. 2). We removed ions deposited as atmospheric inputs based on published data on dissolved loads in Cuban rainfall (Préndez et al., 2014). We then determined evaporite weathering rates by balancing Na with Cl and Ca with SO_4 . The remaining Na was used to
565 determine the silicate contribution of Mg and Ca by using an assumed ratio of Na/Mg of 0.25 and

Na/Ca of 0.35 (Erlanger et al., 2021). Silicate weathering rates were calculated as the total of SiO₂ and HPO₄, assumed to result from silicate weathering. Finally, we balanced the remaining Mg and Ca with bicarbonate to determine carbonate weathering rates.

Considering a variety of landscape-scale metrics, we explored the relationship between ¹⁰Be-derived erosion rates and calculated rock dissolution (total and silicate, carbonate, and evaporite) rates using linear correlations and their associated p-values. All reported means of sample populations are arithmetic.

5 Results

Quartz sand, isolated from central Cuban river sediment, has high concentrations of cosmogenic nuclides (0.41 to 12.6 x 10⁵ atoms g⁻¹ ¹⁰Be and 0.27 to 5.9 x 10⁶ atoms g⁻¹ ²⁶Al). ²⁶Al/¹⁰Be ratios (Fig. 4, Table 1) vary considerably, ranging from 3.65-8.36 (mean = 5.72±1.14, median = 5.83). Sixteen of 24 samples plot below the window defined by continuous exposure and steady erosion on the two-isotope diagram (Fig. 5). Because these ²⁶Al/¹⁰Be data indicate significant burial of quartz during and/or after exposure, many central Cuban drainage basins do not meet the assumption of insignificant nuclide decay inherent in calculations of erosion rates from cosmogenic nuclide concentrations in detrital sediment (Bierman and Steig, 1996). To minimize the impact of violating this assumption, we compare erosion rates based only on the longer-lived nuclide, ¹⁰Be, with landscape scale metrics and dissolved loads. The ¹⁰Be rates, because they cannot properly account for loss of nuclides during burial for samples with depressed ²⁶Al/¹⁰Be ratios, are overestimates of the true rate of erosion.

Erosion rates (Supplement T8), calculated from measured concentrations of ¹⁰Be (Supplement T7), differed considerably between sites. ¹⁰Be-derived erosion rates (Fig. 3) range from 3.4-189 Mg km⁻² y⁻¹ (mean = 59±52, median = 45). Considered as bedrock lowering rates by assuming a bedrock density of 2.6 g cm⁻³, these are 1.3-73 m/My (mean = 23±20, median = 17). ¹⁰Be-derived erosion rates in central Cuba are weakly and positively correlated with mean annual precipitation and slope (Fig. 6). Quartz yields for the samples we analyzed varied widely (0.5%-60%, mean = 20%, median = 17%) but

Formatted: Don't adjust right indent when grid is defined, Line spacing: 1.5 lines, Don't snap to grid

Deleted: We compare measured sediment generation rates to rock dissolution rates (inferred from measurements of dissolved loads in stream water) for the same basins. Across the literature, there is little consensus on calculating chemical weathering rates, with the greatest difference reflecting which elements are included as part of the total dissolved solids (TDS) term (Rad et al., 2013). In our study area, the calculation of rock dissolution rates is further complicated by the variety of underlying rock types present in sampled basins (Supplement T2), which contribute different major ions as t... [47]

Formatted: Font: 12 pt

Deleted: Sediment generation

Deleted: ²⁶Al and

Formatted: Font color: Text 1

Deleted:)

Formatted: Font color: Text 1

Formatted: Font color: Text 1

Deleted:)

Formatted: Font color: Text 1

Deleted: sediment generation

Formatted: Font color: Text 1

Deleted: 7-182 tons

Formatted: Font color: Text 1

Deleted: year

Formatted: Font color: Text 1

Deleted: 53

Formatted: Font color: Text 1

Deleted: 41

Formatted: Font color: Text 1

Formatted: Font color: Text 1

Deleted: 4-70 m/My (mean = 23±21, median = 16) for ¹⁰Be... [48]

Formatted: Font color: Text 1

Deleted: 19

Formatted: Font color: Text 1

Deleted: 21) for ²⁶Al, ²⁶Al/¹⁰Be ratios (Fig. 4) also

Moved (insertion) [3]

Formatted: Font color: Text 1

Formatted: Font color: Text 1

Deleted: considerably, ranging from 2.89-8.32 (

Formatted: Font color: Text 1

Deleted: 5.7±1.2,

Formatted: Font color: Text 1

570 were not significantly correlated ($p < 0.05$) with any basin-scale variables or analytic results (Supplement T1).

575 Rock dissolution rates (Fig. 3) range from $10\text{-}176 \text{ Mg km}^{-2} \text{ y}^{-1}$ (mean = 92 ± 39 , median = 97) and are higher than ^{10}Be -derived erosion rates in 18 of the 23 basins in which we were able to make both measurements. The median rock dissolution rate is 2.15 times higher than the median ^{10}Be -derived erosion rate. Rock dissolution rates and ^{10}Be -derived erosion rates are not correlated (Fig. 6). However, when total rock dissolution rates are partitioned into silicate, evaporite, and carbonate rates then the silicate dissolution rate is positively correlated with ^{10}Be -determined rates of erosion ($r^2 = 0.18$, $p < 0.05$, Table 2). Rock dissolution rates are not separable by dominant basin lithology. ^{10}Be -inferred erosion rates are metamorphic > sedimentary, igneous > sedimentary (Fig. 4).

580 There is lithological dependence of ^{10}Be -derived erosion rates and the ratio of rock dissolution to ^{10}Be -derived erosion rates at the basin scale (Fig. 5). ^{10}Be -derived erosion rates of sedimentary rocks were lower than other rock types ($p = 0.01$). Samples with the lowest $^{26}\text{Al}/^{10}\text{Be}$ ratios and the highest ^{10}Be concentrations (Fig. 5) were collected in the north-western part of the field area in basins predominately underlain by sedimentary rocks (Fig. 2). For the most part, samples from basins 585 dominantly underlain by igneous and metamorphic rocks plot to the left on the two-isotope diagram and have higher $^{26}\text{Al}/^{10}\text{Be}$ ratios than quartz from basins underlain by sedimentary rocks. Basins draining primarily sedimentary lithologies have the highest ratio of rock dissolution to ^{10}Be -derived erosion rates. Seven basins (CU-106, 119, 120, 121, 122, 131, and 132) stand out from the rest (Fig. 5) and are clustered in the northwestern part of our field area. These basins have much lower than average ^{10}Be - 590 derived erosion rates ($3.4\text{-}14.5 \text{ Mg km}^{-2} \text{ y}^{-1}$), low $^{26}\text{Al}/^{10}\text{Be}$ ratios (3.80-5.87), and rock dissolution rates 1.7- 29 times higher than the ^{10}Be -derived rates of erosion. All but CU-131 are underlain primarily by sedimentary rocks.

Neon isotope measurements (Supplement T10) revealed high total neon concentrations with isotope composition indistinguishable from atmosphere, so excess ^{21}Ne was indistinguishable from zero 595 and could not be quantified. Expected cosmogenic ^{21}Ne concentrations in the samples we analyzed, calculated from observed ^{10}Be concentrations and the assumption of steady erosion ($3\text{-}6 \text{ M atoms g}^{-1}$ cosmogenic ^{21}Ne), would comprise less than 2% of the total amount of ^{21}Ne we observed and would not

Deleted: 6.9).

Formatted: Font color: Text 1

Deleted: 24-154 tons

Deleted: 84 ± 34

Deleted: 78

Formatted: Font color: Text 1

Formatted: Don't adjust right indent when grid is defined, Line spacing: 1.5 lines, Don't snap to grid

Deleted: year

Formatted: Font color: Text 1

Formatted: Font color: Text 1

Formatted: Font color: Text 1

Deleted: cosmogenic nuclide

Formatted: Font color: Text 1

Deleted: 16

Formatted: Font color: Text 1

Formatted: Font color: Text 1

Deleted: were made

Formatted: Font color: Text 1

Deleted: 1.4X

Formatted: Font color: Text 1

Deleted: sediment generation rate.

Formatted: Font color: Text 1

Formatted: Don't adjust right indent when grid is defined, Line spacing: 1.5 lines, Don't snap to grid

Deleted: unusually

Deleted: likewise

Deleted: .

be detectable at typical measurement uncertainties. The neon isotope measurements are not inconsistent with the ^{26}Al and ^{10}Be data, but provide no additional information.

6 Discussion

In central Cuba, erosion rates inferred from the concentration of ^{10}Be in river sand vary by more than an order of magnitude. The lowest ^{10}Be -inferred erosion rate ($3.4 \text{ Mg km}^{-2} \text{ y}^{-1}$; 1.3 m/My) is less than those measured in tectonically stable arid landscapes including Namibia and Australia (White et al., 1998; Von Blackenburg et al., 2004; Salgado et al., 2006; Regard et al., 2016). The highest ^{10}Be -inferred rate ($189 \text{ Mg km}^{-2} \text{ y}^{-1}$; 73 m My^{-1}) exceeds those measured in temperate, humid, tectonically stable areas such as the southern Appalachian Mountains (Portenga et al., 2019; Duxbury et al., 2015; Linari et al.) and is similar to or less than rates measured on other Caribbean Islands including Puerto Rico and Dominica (Quock et al., 2021; Brocard et al., 2015; Brown et al., 1995b).

Variability in ^{10}Be concentration, and thus inferred rates of erosion, between central Cuban drainage basins, many within just a few tens of kilometers of each other with similar basin slope, suggests significant landscape-scale controls on ^{10}Be concentration and thus mass loss. Indeed, we find that ^{10}Be -determined erosion rates are positively correlated with slope ($R^2=0.20$, $p=0.03$), mean annual precipitation ($R^2=0.22$, $p=0.02$), and rates of silicate dissolution ($R^2=0.17$, $p=0.05$) (Fig. 6, Table 2). Erosion rates are lowest for basins underlain dominantly by sedimentary rocks and highest for basins underlain by metamorphic rocks (Fig. 3). However, accurately quantifying rates of denudation (total mass loss) from central Cuban landscapes is complicated by significant export of mass in solution and near-surface quartz enrichment. In the sections that follow, we discuss the ^{10}Be data in the context of dissolved load export in river water and the landscape-scale insight on active processes provided by dual-isotope measurements (^{26}Al and ^{10}Be) made in riverine quartz.

6.1 Cosmogenic erosion rates underestimate landscape scale mass loss in Cuba

Our data show clearly that significant, landscape-scale mass loss is occurring by solution in central Cuba. Rock dissolution rates exceed, some by more than an order of magnitude, corresponding

Deleted: Thus, the

Deleted: do not

Deleted: any

Deleted: useful

Deleted: There is lithological dependence of both sediment generation rates and rock dissolution rates at the basin scale (Fig. 5). Basins draining primarily sedimentary lithologies had the highest rock dissolution rates and the lowest sediment generation rates; this trend was reversed in basins draining primarily metamorphic lithologies. The sediment generation rates of sedimentary rocks were lower than the sediment generation rates of other rock types ($p = 0.02$). Quartz yields (0.5%-60%, mean = 20%, median = 27%) were not correlated with any basin-scale variables (Supplement F1). Sediment generation

Moved up [3]: rates in central Cuba are weakly and positively correlated with mean annual precipitation and slope (Fig. 6).

Deleted: Rock dissolution rates and sediment generation rates are not correlated (Fig. 7). The $^{26}\text{Al}/^{10}\text{Be}$ ratios of basins underlain by sedimentary rocks are distinctly lower than the ratios observed in basins underlain by metamorphic rocks ($p=0.001$). Several basins (CU-106, 120, 121, 122, and 132) have much lower than average sediment generation rates ($3.7\text{-}11 \text{ tons km}^{-2} \text{ year}^{-1}$), plot near each other outside of the simple exposure region on the right of the two-isotope diagram with low $^{26}\text{Al}/^{10}\text{Be}$ ratios (3.80-5.09), and have rock dissolution rates 9-32X higher than the sediment generation rates. The rock dissolution rates in two additional basins (CU-016 and 131) are 3.6-6X higher than their respective sediment generation rates; all also plot on the right side of the two-isotope diagram, and CU-016 falls far below the simple exposure region, with a $^{26}\text{Al}/^{10}\text{Be}$ ratio of 2.89 (Fig. 4).

Formatted: Font color: Text 1

Formatted: Font: 12 pt

Deleted: 6.1 Discordance between high rock dissolution

Formatted: Font color: Text 1, English (US)

Deleted: and low sediment generation rates
Rock dissolution rates exceed, sometimes

Formatted: Font color: Text 1

Formatted: Font color: Text 1

Deleted: , most corresponding sediment generation rates in Cuba, demonstrating that the cosmogenic nuclide measurements are an incomplete assessment of total mass loss from the landscape. This comparison shows that mass loss

Formatted: Font color: Text 1

Deleted: occurring largely by solution

Formatted: Font color: Text 1

Deleted: central Cuba, which is consistent with observations from other tropical

Formatted: Font color: Text 1

Formatted: Font color: Text 1

¹⁰Be-derived mass loss rates in central Cuba, demonstrating that the cosmogenic nuclide measurements are an incomplete assessment of total mass loss from the landscape. Rock dissolution rates are greater than cosmogenic erosion rates for 18 of the 23 basins we analyzed and the median rock dissolution rate in Cuba is 2.15 times higher than median cosmogenic nuclide-derived rate (Table 1, Fig. 7). Rock dissolution rates that significantly exceed corresponding ¹⁰Be-inferred rates have also been reported from Uganda (Hinderer et al., 2013) and Cameroon (Regard et al., 2016), where they were attributed to the influence of easily weathered volcanic tephra and deep weathering associated with thick regolith, respectively. Most other studies that compare rock dissolution rates and ¹⁰Be-derived erosion rates in the tropics documented rock dissolution rates within the range of cosmogenic nuclide-derived rates (Von Blackenburg et al., 2004; Salgado et al., 2006; Cherem et al., 2012; Sosa Gonzalez et al., 2016b; Quock et al., 2021). Cuba is different.

The discordance between high rock dissolution rates and low ¹⁰Be-derived erosion rates in central Cuba suggests that significant rock weathering is occurring below the depth of most cosmogenic nuclide production (Bierman and Steig, 1996; Fig. 1). The discordance, along with high rates of carbonate and evaporite dissolution in some basins, suggests that many lithologies in our field area are highly susceptible to dissolution. Bierman et al. (2020) attribute high rock dissolution rates and the relationship between stream water chemistry and bedrock type in central Cuba to extensive rock-groundwater interaction along subsurface flow paths, controlled by ongoing bedrock uplift and associated rock fracturing. The prevalence of rock dissolution at depth in Cuba is consistent with findings from other humid, tropical landscapes, including Puerto Rico (White et al., 1998; Kurtz et al., 2011; Chapela Lara et al., 2017; Moore et al., 2019), Guadeloupe, Martinique, Dominica (Rad et al., 2007), and Hawaii (Schopka and Derry, 2012).

We observed no correlation between ¹⁰Be-derived erosion and rock dissolution rates in central Cuba (Fig. 7), in contrast to other studies in the tropics that have observed generally positive correlations (Salgado et al., 2006; Cherem et al., 2012; Sosa Gonzalez et al., 2016b) The lack of correlation suggests that mass loss below several meters, the depth at which most cosmogenic nuclides are produced, is an important component of denudation in Cuba. Discordance between high rock dissolution rates and low ¹⁰Be-derived erosion rates observed in Cuba occurs in basins with different

underlying lithologies (Fig. 6). Such widespread discordance suggests deep chemical weathering is occurring throughout central Cuba.

Carbonate weathering dominates river water geochemistry in central Cuba. Our analysis of Cuban water composition suggests that the rate of carbonate dissolution varies widely and in most basins we sampled, exceeds by several-fold the rate of silicate dissolution (Fig. 4). Silicate dissolution rates are low ($<25 \text{ Mg km}^{-2} \text{ y}^{-1}$) and similar between all lithologies. Export rates of elements calculated to reflect the presence of evaporite minerals are also generally low ($<35 \text{ Mg km}^{-2} \text{ y}^{-1}$), except in four basins dominated by sedimentary rocks (CU-120, 121, 122, 132). Water geochemistry data from four of these basins suggest the presence of significant evaporite deposits due to high concentrations of Cl, SO_4 , Br, and Na (Bierman et al., 2020). Together these data imply that lithologies underlying the basins we sampled are not uniform and that silicate rocks do not account for most of the dissolved mass loss in at least some, and likely many, of the basins we sampled.

Together, underlying lithology and topography are important controlling factors in how and how rapidly the Cuban landscapes we studied are losing mass by both physical and chemical weathering. Lowland basins, primarily underlain by sedimentary rocks, on average have low rates of ^{10}Be -inferred mass loss and high rates of dissolution. Six basins underlain by sedimentary lithologies (CU-106, -119, -120, -121, -122, and -132) have the highest ^{10}Be concentrations and lowest erosion rates indicating longer total exposure durations for the quartz we analyzed. All are low slope (0.5 to 1.6 degrees). These six basins also demonstrate the greatest disparity between high rock dissolution rates and low ^{10}Be -derived erosion rates (5.7-29X). One basin underlain by igneous rocks (CU-131) has similarly low slope (0.6 degrees) and high ^{10}Be concentration but a much lower ratio of dissolution to erosion rates (1.7) likely reflecting the paucity of readily soluble minerals. As a result, ^{10}Be -derived erosion rates are weakly and positively correlated with average basin slope ($R^2 = 0.20$, $p=0.03$), but rock dissolution rates are not correlated ($R^2 = 0.04$, $p=0.36$) with slope.

Moved down [4]: 6.2 Low $^{26}\text{Al}/^{10}\text{Be}$ ratio evidence for a deep mixed surface layer and possible quartz enrichment

Deleted: The predominance of rock dissolution in these landscapes is likely a reflection of the favorable weathering conditions created by tropical climates (Pope, 2013). In areas with slow physical erosion, chemical export is also favored (Anderson et al., 2007).

Underlying basin rock type and topography are important controlling factors in how and how rapidly the Cuban landscapes we studied are denuding. Correlations between rock dissolution and sediment generation rates with basin slope and elevation are influenced by the distribution of lithologies in our study area, as low-relief, soluble sedimentary rocks are concentrated at low elevations, and steeper, less soluble metamorphic rocks are concentrated at higher elevations. Whereas sediment generation rates are weakly and positively correlated with average basin slope ($p=0.10$, $R^2 = 0.13$), rock dissolution rates are strongly negatively correlated ($p=0.01$, $R^2 = 0.27$) with slope. Rock dissolution rates are also negatively correlated ($p=0.01$, $R^2 = 0.24$) with average elevation. Rock type plays a key role in determining rock dissolution rates as well. Rock dissolution rates are highest in the low elevation, low slope basins underlain primarily by sedimentary rocks, and lowest in the steeper, high elevation metamorphic basins—the opposite trend observed in sediment generation rates. These trends emphasize the importance of low-relief topography and the availability of soluble rocks in driving the rate of rock dissolution in Cuba.

While most other studies that compare rock dissolution rates and sediment generation rates in the tropics documented rock dissolution rates within the range of cosmogenic nuclide-derived rates (Von Blackenburg et al., 2004; Salgado et al., 2006; Cherem et al., 2012; Sosa Gonzalez et al., 2016b), the mean rock dissolution rate in Cuba is 6X higher than corresponding cosmogenic nuclide-derived rates. Rock dissolution rates that significantly exceed corresponding ^{10}Be -inferred rates have been observed in Uganda (Hinderer et al., 2013) and Cameroon (Regard et al., 2016), where they were attributed to the influence of easily weathered volcanic tephra and deep weathering associated with thick regolith, respectively. As the discordance between high rock dissolution rates and low sediment generation rates observed in Cuba occurs in basins with different underlying lithologies, the disagreement between these rates suggests deep chemical weathering is occurring throughout central Cuba regardless of lithology.

The contrast between high rock dissolution rates and low sediment generation rates suggests that significant rock weathering is occurring below the depth of most cosmogenic nuclide production (Bierman and Steig, 1996; Fig. 1). Bierman et al. (2020) attribute high rock dissolution rates and the relationship between stream water chemistry and bedrock type in Cuba to extensive rock-groundwater interaction along subsurface flow paths, controlled by ongoing bedrock uplift and associated rock fracturing. The strong negative correlation between chemical denudation rates and average basin slope also supports the importance of deep weathering in landscape denudation, since such weathering occurs when rock dissolution progresses faster than weathering products are removed from the landscape, a process favored in low relief settings (Ollier, 1988). In contrast to other studies in the tropics that have ob...

Formatted: Font color: Text 1

Formatted: Font color: Text 1,

Deleted: $^{26}\text{Al}/$

Formatted: Font color: Text 1

6.2 Low $^{26}\text{Al}/^{10}\text{Be}$ ratio evidence for a deep mixed surface layer and possible quartz enrichment

The $^{26}\text{Al}/^{10}\text{Be}$ ratios suggest that most sediment we collected from central Cuban rivers does not have a simple exposure history. $^{26}\text{Al}/^{10}\text{Be}$ data in 16 of 24 sampled basins are inconsistent with steady surface erosion (Fig. 5). Many of the basins with the lowest $^{26}\text{Al}/^{10}\text{Be}$ ratios drain predominantly marine sedimentary lithologies, and have low average basin slopes (0.5-0.7°); the remaining basin drains primarily igneous rocks and has an average basin slope of 0.6°. These are the same seven basins discussed in the section above, all but one of which have high ratios of dissolved load to ^{10}Be -inferred erosion rates. There is a significant ($R^2 = 0.34$, $p = 0.003$) relationship between average basin slope and $^{26}\text{Al}/^{10}\text{Be}$.

Observed $^{26}\text{Al}/^{10}\text{Be}$ ratios in most of the low-ratio samples are consistent with bioturbation and prolonged near-surface exposure (Struck et al., 2018). We suspect that at least some of the inconsistency between measured $^{26}\text{Al}/^{10}\text{Be}$ ratios and those predicted by a simple steady-state surface erosion model is due to (deep) soil mixing. Typically, the lower boundary of the simple exposure region of a two-isotope diagram (Fig. 5) is constructed based on the assumption that all grains move monotonically towards the surface at the rate that the surface is eroding (Granger, 2006). Vertical mixing, due to bioturbation or other soil processes taking place in the upper layers of soil, violates this assumption. Within a mixed soil layer, grains circulate at a higher velocity than the erosion rate, and therefore experience an average production rate lower than the surface rate and spend time below the surface where the rate of nuclide decay may exceed the rate of nuclide production. During burial, $^{26}\text{Al}/^{10}\text{Be}$ ratios decrease and diverge from those predicted by the steady-state surface erosion model (Fig. 5).

Rapid chemical mass loss due to the presence of readily soluble evaporite and marine or igneous lithologies in some basins likely enriches the remaining sediment in quartz. The combination of mass loss by rapid rock dissolution and the retention of weathering residuum favored by subdued topography in low-relief basins allows less-soluble material (e.g., quartz) to accumulate at and near the surface, creating thick regolith. Extensive vertical mixing of near-surface soil, as is expected for flat, forested landscapes where the rate of bioturbation is likely high in relation to slow erosion rates, leads to longer

Moved (insertion) [4]

Formatted ... [50]

Formatted ... [52]

Formatted ... [51]

Formatted ... [53]

Deleted: data in seven

Formatted ... [54]

Deleted: 4). The basin with the lowest $^{26}\text{Al}/^{10}\text{Be}$ ratio (CU ... [55]

Formatted ... [56]

Deleted: sample

Formatted ... [57]

Deleted: volcanic

Formatted ... [58]

Deleted: These six basins underlain by marine or volcanic ... [59]

Formatted ... [61]

Deleted: six

Formatted ... [62]

Deleted: seven

Formatted ... [63]

Formatted ... [60]

Deleted: (all except CU-016) can be explained by

Formatted ... [64]

Deleted: (Struck et al., 2018)

Formatted ... [65]

Deleted: 4

Formatted ... [66]

Deleted: (Granger, 2006)

Formatted ... [67]

Deleted: both a different

Formatted ... [68]

Deleted: assumed by a simple steady

Formatted ... [69]

Deleted: erosion model

Formatted ... [70]

Deleted: buried.

Formatted ... [71]

Deleted: lower

Formatted ... [72]

Deleted: thus

Formatted ... [73]

Deleted: a simple

Formatted ... [74]

Deleted: .

Formatted ... [75]

Deleted: denudation

Formatted ... [76]

Deleted: volcanic deposits

Formatted ... [77]

Deleted: these six

Formatted ... [78]

Deleted: of

Formatted ... [79]

Deleted: due to soluble deposits

Formatted ... [80]

Deleted: low

residence times for these residual mineral grains, and therefore a lower $^{26}\text{Al}/^{10}\text{Be}$ ratio, in a mixed surface layer compared to a surface eroding at the same rate without vertical mixing.

This assertion is supported by the consistency between measured $^{26}\text{Al}/^{10}\text{Be}$ ratios and expected nuclide concentrations and ratios calculated assuming the presence of a mixed surface layer (per Lal and Chen (2005), equation 12). Expected $^{26}\text{Al}/^{10}\text{Be}$ ratios calculated assuming a mixed layer depth of 40-160 cm agree well with measured low $^{26}\text{Al}/^{10}\text{Be}$ ratios from basins CU-119, CU-122 and 132 (Fig. 5). This mixed layer depth range is consistent with the soil depths of 90-150 cm reported for the location of these basins (Bennett and Allison, 1928). In deeply weathered tropical soils, bioturbation can extend to depths of several meters (Von Blackenburg et al., 2004), so it is plausible that mixing depths are even greater than the model suggests, providing an explanation for the $^{26}\text{Al}/^{10}\text{Be}$ ratios measured in CU-120, 121, 131, and 106. We were not able to measure regolith depths in the drainage basins we sampled.

The $^{26}\text{Al}/^{10}\text{Be}$ ratio in other samples (e.g., CU-106, 118, and 110) is too low to be attributed solely to the effects of a deep mixed surface layer, and requires that some fraction of the sample has experienced both surface exposure and a significant period of burial well below the surface where cosmogenic nuclide production is negligible. Factors that could lead to this low ratio include the incorporation of previously deeply buried sediment through channel avulsion (Wittmann et al., 2011) or incision into terraces (Hu et al., 2011). We conclude terrace storage, along with a combination of quartz enrichment due to high chemical weathering rates of soluble marine rocks in combination with very low slope basins and a deep mixing layer, combine to generate detrital quartz with high concentrations of ^{10}Be and lower than expected $^{26}\text{Al}/^{10}\text{Be}$ ratios.

6.3 Constraining total rates of landscape denudation

The disagreement between high rock dissolution rates and low ^{10}Be -derived erosion rates raises questions about how to best characterize total landscape denudation rates. It is clear from our data set that neither cosmogenic nuclide measurements nor stream solute flux are capturing all or even, in some cases, the majority of landscape denudation in central Cuba. Evidence for deep rock dissolution presented in section 6.1 suggests that sediments and solutes are being sourced at least partially from

Formatted: Font color: Text 1

Deleted: mixed

Formatted: Font color: Text 1

Formatted: Font color: Text 1

Deleted: Lal and Chen (2005)

Formatted: Font color: Text 1

Deleted: .

Formatted: Font color: Text 1

Formatted: Font color: Text 1

Deleted: (Bennett and Allison, 1928).

Formatted: Font color: Text 1

Deleted: 3-4 m (Von Blackenburg et al., 2004)

Formatted: Font color: Text 1

Deleted: . Access restrictions in Cuba prevent us from directly measuring ...

Formatted: Font color: Text 1

Formatted: Font color: Text 1

Deleted: the lowest-ratio sample (CU-016)

Formatted: Font color: Text 1

Deleted: (Wittmann et al., 2011) or incision into terraces (Hu et al., 2011). However, satellite image analysis does not provide compelling evidence, such as incised terraces, for the presence of previously exposed then deeply buried material. Extensive subsurface dissolution leads to the observed and significant disagreement between slow sediment generation rates and fast rock dissolution rates. The lengthy exposure durations inferred from high ^{10}Be concentrations in quartz from CU-106, 120, 121, 122, 131, and 132 demonstrate that even in the high-precipitation, tropical environment of central Cuba, quartz can remain stable, with long residence times in the landscape of low-slope basins. However, this cannot be the entire story because ... [83]

Deleted: that

Formatted: Font color: Text 1

Formatted: Font: 12 pt, Font color: Text 1

Formatted: ... [84]

Formatted: Font: 12 pt, Font color: Text 1

Formatted: Font color: Text 1

Formatted: ... [85]

Deleted: sediment generation

Formatted: Font color: Text 1

Deleted: , since

Formatted: Font color: Text 1

Formatted: Font color: Text 1

different depths in the landscape. Because most mass loss in much of central Cuba occurs in solution (rock dissolution rates are higher than ¹⁰Be-derived erosion rates in 18 of 23 basins), rock dissolution rates typically represent a minimum bound on total landscape denudation.

Treating the removal of mass in solution and through physical erosion as entirely discrete processes happening at different depths in the landscape sets an upper limit on total landscape denudation: the sum of inferred rock dissolution rates and ¹⁰Be-derived erosion rates. Summing ¹⁰Be-derived erosion rates and chemical denudation rates increases estimates of total landscape denudation across study basins by a factor of 1.4-30 (mean = 6.3, median = 2.7) above ¹⁰Be-derived erosion rates.

Disregarding the six basins with evidence of evaporite deposits (CU-106, -119, -120, -121, -122, and -132) leads to an average increase of a factor of 2.6 (median = 2.5) above ¹⁰Be-derived erosion rates.

These mean and median values for the basins without evaporites are between the reported CEF of 1.79 for the Luquillo Critical Zone Observatory in humid, tropical Puerto Rico (Riebe and Granger, 2013) and the CEF of 3.2 for the thickly saprolite-mantled, tropical environment of south Cameroon (Regard et al., 2016). These comparisons suggest that for landscapes with a significant proportion of total denudation occurring through deep rock dissolution, summing rock dissolution rates and cosmogenic nuclide-derived rates provides a reasonable estimate of total landscape denudation.

In landscapes like central Cuba, total denudation rates may be difficult to predict based on landscape metrics. Summed chemical denudation rates and cosmogenic nuclide-derived erosion rates are not correlated with rock type, as rock type appears to have opposing influences on these rates (i.e., basins underlain by sedimentary rocks had the highest rock dissolution rates but lowest cosmogenic nuclide-derived rates, Fig. 3). Summed rock dissolution rates and cosmogenic nuclide-derived rates do increase with mean basin slope ($R^2=0.19$, $p=0.04$) and mean basin elevation ($R^2=0.17$, $p=0.05$) (Fig. 5), but those relationships are confounded because ¹⁰Be-derived rates are highest in high elevation, steep basins and rock dissolution rates are highest in low slope, low elevation basins—relationships that are primarily controlled by the influence of rock type on these two different mass loss processes.

In central Cuba, the lack of correlation between rock dissolution rates and ¹⁰Be-derived erosion rates (Fig. 7) suggests a possible mechanism for limiting total reduction in landscape relief. While global data demonstrates significant, positive correlations between ¹⁰Be-derived erosion rates and basin

Deleted: Since it is clear that the majority of

Formatted ... [86]

Deleted: sediment generation

Formatted ... [87]

Deleted: most

Formatted ... [88]

Formatted ... [89]

Deleted: allows us to set a maximum bound

Formatted ... [90]

Deleted: sediment generation

Formatted ... [91]

Deleted: In basins with evidence of evaporite deposits, th

Formatted ... [92]

Formatted ... [93]

Deleted: sediment generation

Formatted ... [94]

Deleted: 33

Formatted ... [95]

Deleted: 4

Formatted ... [96]

Deleted: 5

Formatted ... [97]

Deleted: sediment generation

Formatted ... [98]

Deleted: extreme examples of the

Formatted ... [99]

Deleted: 8

Formatted ... [100]

Deleted: 2

Formatted ... [101]

Deleted: sediment generation

Formatted ... [102]

Deleted: (Riebe and Granger, 2013)

Formatted ... [103]

Deleted: (Regard et al., 2016).

Formatted ... [104]

Deleted:). Similarly, summed

Formatted ... [105]

Deleted: are not correlated

Formatted ... [106]

Deleted: or mean basin slope (Fig. 6), since ¹⁰Be

Formatted ... [107]

Deleted: were

Formatted ... [108]

Deleted: were

Formatted ... [109]

Deleted: denudational

Formatted ... [110]

Deleted: summed

Formatted ... [111]

Deleted: sediment generation

Formatted ... [112]

Deleted: reductions

Formatted ... [113]

Deleted: sediment generation

Formatted ... [114]

slope and relief (Portenga and Bierman, 2011), accounting for the influence of rock dissolution may alter this dynamic. The possibility of combined physical and chemical processes limiting reductions in relief has significant implications for the study of deeply weathered, high-relief tropical landscapes. The dual importance of rock dissolution in low-lying areas and physical erosion in steeper terrain could explain the relationship behind sustained high relief topography and low ¹⁰Be-derived erosion rates common across some tropical landscapes, such as Brazil (Vasconcelos et al., 2019) or Sri Lanka (Von Blackenburg et al., 2004). Landscapes with high rock dissolution rates and low physical erosion rates appear to be relatively common (Larsen et al., 2014b). As lowlands weather primarily through rock dissolution and high relief areas by physical erosion, total relief would change more slowly than ¹⁰Be-estimated rate differentials would suggest.

Regardless of rock type, however, cosmogenic nuclide-derived erosion rates are positively correlated with MAP ($R^2 = 0.22$, $p = 0.02$). While MAP does not vary widely across our study basins in central Cuba (956 to 1555 mm y^{-1}), this correlation suggests a climatic control on denudation rates across this landscape. This finding is contrary to other studies in the humid tropics (Von Blackenburg et al., 2004), and beyond (Riebe et al., 2001b; Portenga and Bierman, 2011), that have found no correlation between climate variables and cosmogenic nuclide-derived long-term erosion rates but similar to recent findings in humid, temperate Tasmania (Vanlandingham et al., 2022). Since in Cuba ¹⁰Be-derived erosion rates are positively correlated with MAP but chemical denudation rates are uncorrelated with MAP, this trend likely highlights the importance of rainfall in allowing for the physical export of sediment from a drainage basin that is transport-limited rather than weathering-limited.

Our data clearly demonstrate that cosmogenic nuclide measurements can underestimate total denudation in landscapes with significant rock dissolution at depth, particularly in the tropics. This suggests that similar underestimates of total denudation rates produced by relying on measurements of cosmogenic nuclides may be a factor in other tropical landscapes. While rock dissolution rates in the tropics have been documented as among the highest globally (White and Blum, 1995; Rad et al., 2013; Larsen et al., 2014a), a global compilation of ¹⁰Be-derived erosion rates demonstrated that such isotopically determined rates of erosion are lower in the tropics than in all other climate zones, apart

- Deleted: (Portenga and Bierman, 2011)
- Formatted ... [115]
- Deleted:
- Formatted ... [116]
- Deleted: sediment generation
- Formatted ... [117]
- Deleted: (Vasconcelos et al., 2019)
- Formatted ... [118]
- Deleted: (Von Blackenburg et al., 2004)
- Formatted ... [119]
- Deleted: are weathering
- Formatted ... [120]
- Deleted: are weathering primarily through sediment generation
- Formatted ... [121]
- Deleted: remain relatively unchanged
- Formatted ... [122]
- Deleted: both
- Formatted ... [123]
- Deleted: and summed chemical denudation rates and cos ... [124]
- Formatted ... [125]
- Deleted: $p = 0.005$,
- Formatted ... [126]
- Deleted: 34
- Formatted ... [127]
- Deleted: /year
- Formatted ... [128]
- Deleted: (Von Blackenburg et al., 2004)
- Formatted ... [129]
- Deleted: (Riebe et al., 2001b; Portenga and Bierman, 2011)
- Formatted ... [130]
- Deleted: correlations
- Formatted ... [131]
- Deleted: .
- Formatted ... [132]
- Deleted: sediment generation
- Formatted ... [133]
- Deleted: , suggesting
- Formatted ... [134]
- Deleted: using
- Formatted ... [135]
- Deleted: (White and Blum, 1995; Rad et al., 2013; Lars ... [136]
- Formatted ... [137]
- Deleted: sediment generation
- Formatted ... [138]
- Deleted: are lower
- Formatted ... [139]

from arid regions (Portenga and Bierman, 2011). The contrast between these two depictions of tropical denudation suggests that ^{10}Be -derived erosion rates for tropical areas may be incomplete representations of total mass loss from these landscapes because dissolved loads are incompletely accounted for by measurements of ^{10}Be in river sand. This discrepancy highlights the need for more studies that compare rock dissolution rates and cosmogenic nuclide-derived rates to provide more accurate estimations of total landscape denudation (Vanlandingham et al., 2022).

7 Conclusions

The first cosmogenic nuclide measurements from the island of Cuba provide insight into how mass is lost from landscapes in humid, tropical settings. Solution plays a large role in total mass flux, and significant mineral dissolution occurs along weathering fronts meters below the landscape surface. Rock type exerts the primary control on the pace of denudation, and precipitation influences rates of landscape change. We find evidence for thick mixed surface layers in lowland basins and river water chemistry data suggest that deep rock dissolution dominates denudational processes in low slope basins where weathering products remain near the surface for long periods of time.

These findings highlight the necessity of accounting for mass loss by solution at depths below the penetration of most cosmic rays when interpreting cosmogenic nuclide-derived rates in landscapes with the potential for significant rock dissolution. The discrepancy between high rock dissolution rates and low ^{10}Be -derived erosion rates observed in central Cuba emphasizes how relying on cosmogenic nuclide measurements alone to determine total rates of mass loss from landscapes can lead to considerable underestimates of denudation. Summing mass loss rates in solution with mass loss rates inferred from cosmogenic nuclides provides an upper limit for total mass loss from landscapes when significant rock dissolution occurs below the penetration depth of cosmic ray neutrons. These findings suggest that estimating rock dissolution rates is important when applying cosmogenic nuclides in landscapes, especially those which are humid, tropical, have soluble rocks, and/or have deep weathered regolith.

Deleted: (Portenga and Bierman, 2011).

Formatted ... [140]

Deleted: are

Formatted ... [141]

Deleted: , in the tropics and beyond,

Formatted ... [142]

Deleted: .

Formatted ... [143]

Deleted: 6.4 Comparison of long-term sediment gener ... [144]

Formatted ... [145]

Deleted: Our data, the

Formatted ... [146]

Deleted: ,

Formatted ... [147]

Deleted: landscape denudation occurs

Formatted ... [148]

Deleted: total

Formatted ... [149]

Deleted: denudation

Formatted ... [150]

Deleted: depth

Formatted ... [151]

Deleted: sediment generation

Formatted ... [152]

Deleted: denudation

Formatted ... [153]

Deleted: underestimations of total mass flux off landscapes.

Formatted ... [154]

Deleted: rock dissolution

Formatted ... [155]

Deleted: and sediment generation

Formatted ... [156]

Deleted: can provide maximum estimates of total denudation in

Formatted ... [157]

Deleted: with

Formatted ... [158]

Deleted: concentrated

Formatted ... [159]

Deleted: to other humid, tropical

Formatted ... [160]

Deleted: where solute fluxes carried in stream loads

Formatted ... [161]

Deleted: significant

Formatted ... [162]

8 Data availability

The data are under review at Pangaea (<https://doi.pangaea.de/10.1594/PANGAEA.940043>).

9 Author contributions

AHS, MKC, and PB contributed to project design. AGA, AGM, AHS, HCA, MKC, PBR, and RSH conducted fieldwork. MKC prepared samples for laboratory analysis. GB, LS, MC, AHS, PRB, and MKC contributed to cosmogenic nuclide analysis. MKC, PRB, and AHS led manuscript preparation; all authors assisted with data analysis and manuscript writing and review. GB, MKC, and AHS prepared the figures. AHS completed the chemical weathering calculations.

10 Competing interests

Some authors are members of the editorial board of Geochronology. The peer-review process was guided by an independent editor, and the authors have no other competing interests to declare.

11 Acknowledgements

Support for fieldwork and analyses provided by NSF EAR-1719249 and NSF EAR-1719240 to Bierman and Schmidt, NSF EAR 1735676 to Bierman, and Oberlin College funding to Schmidt. Researchers from Centro de Estudios Ambientales de Cienfuegos were supported by the MICATIN and ISOAGRI projects. We thank Jay Racela and Marika Massey-Bierman for their assistance with laboratory work, and Marika Massey-Bierman, Monica Dix, Victor Manuel Fonseca Pérez, and Santiago Gil Pérez for assistance with fieldwork. We thank Erica Erlanger and Claire Lukens for constructive reviews. Prepared in part by LLNL under Contract DE-AC52-07NA27344. LLNL-JRNL-824414.

Deleted: ¶

Formatted: Font: 12 pt, Font color: Text 1

Deleted: Data

Formatted: Font: 12 pt, Not Bold, Font color: Text 1, English (US)

Deleted: the

Formatted: Font: 12 pt, Not Bold, Font color: Text 1, English (US)

Deleted: database (PDI-29915).

Formatted: Font: 12 pt, Not Bold, Font color: Text 1, English (US)

Formatted: Font: 12 pt, Font color: Text 1

Formatted: Font color: Text 1

Formatted: Font color: Text 1

Formatted: Font color: Text 1

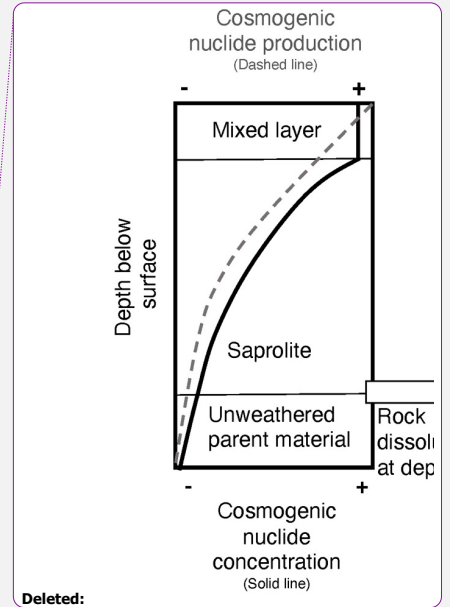
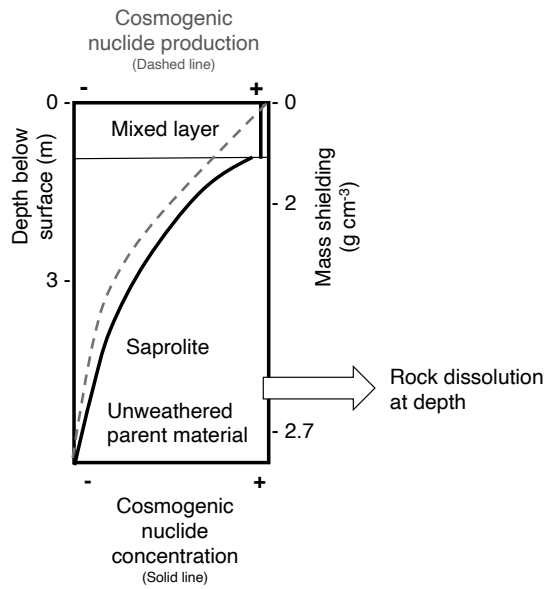
Formatted: Font color: Text 1

Formatted: Font: 12 pt

Deleted: also

Formatted: Font: 12 pt

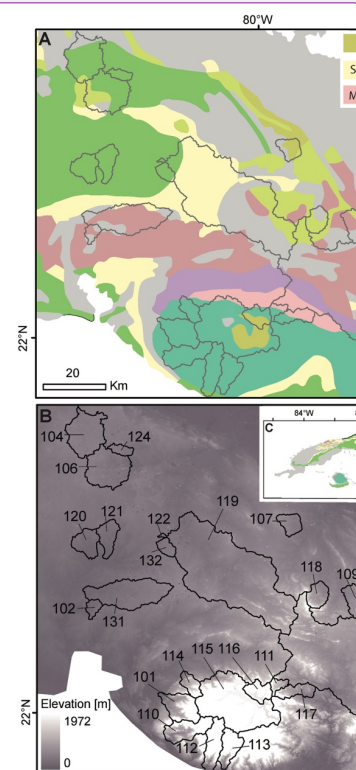
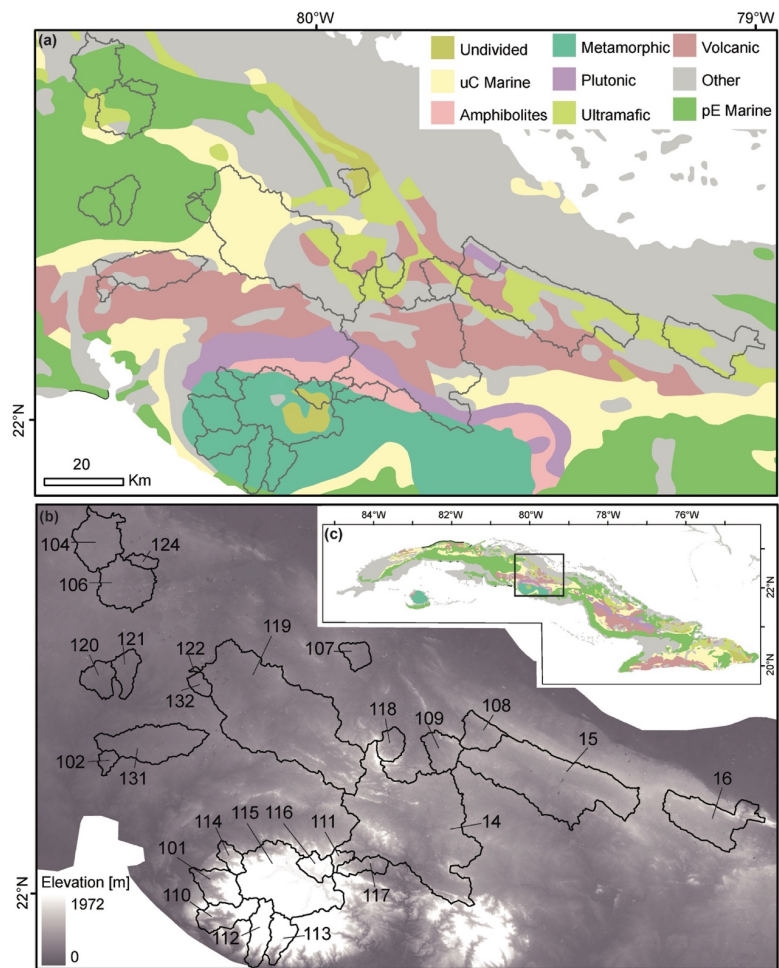
Deleted: and



465

Figure 1: Conceptual diagram showing cosmogenic nuclide production and concentration in a column of soil, saprolite, and rock. The dashed line shows decreasing production of cosmogenic nuclides with depth; solid line shows nuclide concentration with depth, and the white arrow represents mass loss by solution below the depth of significant cosmogenic nuclide production.

Formatted: Font: 12 pt, Not Bold



Deleted:

Formatted: Font: 12 pt

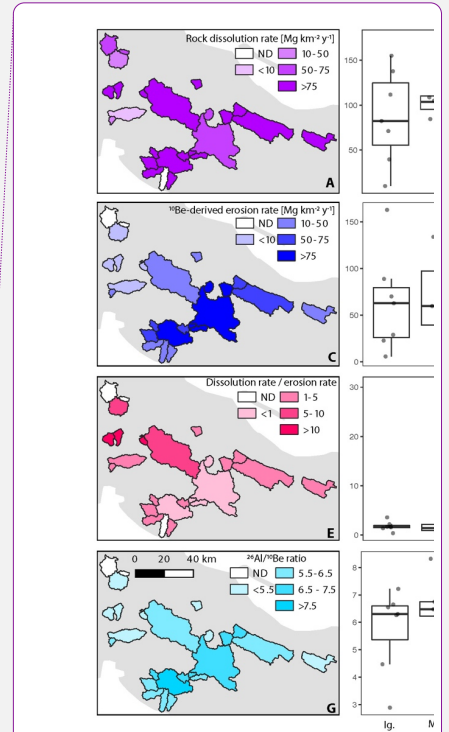
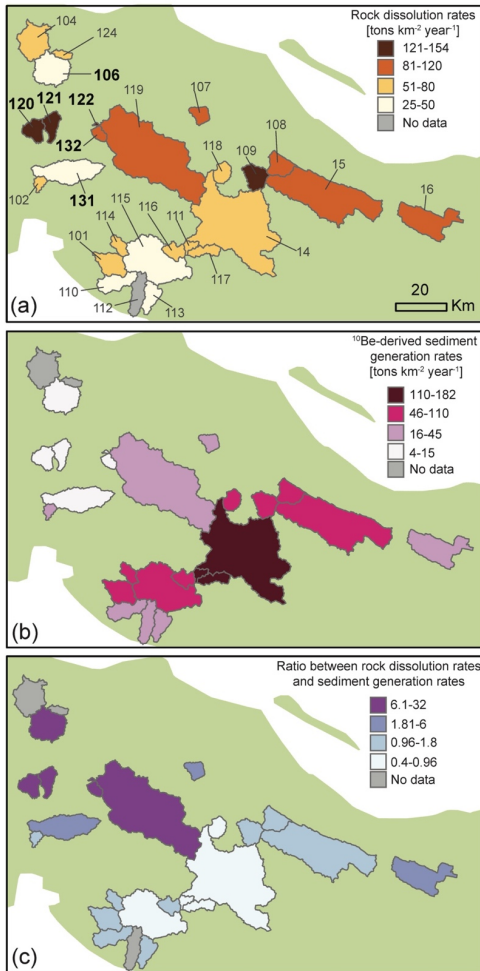
475

Figure 2: Maps showing underlying basin geology (panel A; French and Schenk, 2004), elevations (panel B; Lp Daac), and location of study area within the island of Cuba (panel C). Legend for panel A includes the category of the rock units in terms of sedimentary (S), igneous (I), and metamorphic (M). Note that the two marine units in A are separated because they have different chemical load signatures.

Formatted: Font: 12 pt, Not Bold

Deleted: : Maps showing underlying basin geology (panel A; French and Schenk, 2004), elevations (panel B; LPDAAC), and location of study sites within the island of Cuba (panel C).

Formatted: Font: 12 pt, Not Bold



Deleted:

Formatted: Font: 12 pt

Formatted: Font: 12 pt, Not Bold

Formatted: Font: 12 pt, Not Bold

Deleted: Panel A shows measured sediment generation

Formatted: Font: 12 pt, Not Bold

Deleted: , and panel B shows measured rock dissolution.

Formatted: Font: 12 pt, Not Bold

Figure 3: Maps showing rates of landscape change and isotopic data for each study watershed. A,B. Rock dissolution rates. C,D. ¹⁰Be-derived erosion rates. In both maps, darker colors in the basins

indicate faster rates of landscape change. E.F. Ratio between rock dissolution rates and ^{10}Be -derived erosion rates; darker colors indicate larger ratios. G.H. $^{26}\text{Al}/^{10}\text{Be}$ ratio. Darker colors are higher ratios. Box plots show the maximum and minimum values in the lines extending from the box; the upper side of the box represents the upper quartile, the line inside of the box represents the median value, and the bottom of the box represents the lower quartile. Y axis units are the same as shown in the corresponding map legend.

Deleted: Panel C shows the ratio

Formatted: Font: 12 pt, Not Bold

Deleted: sediment generation

Formatted: Font: 12 pt, Not Bold

Formatted: Font: 12 pt

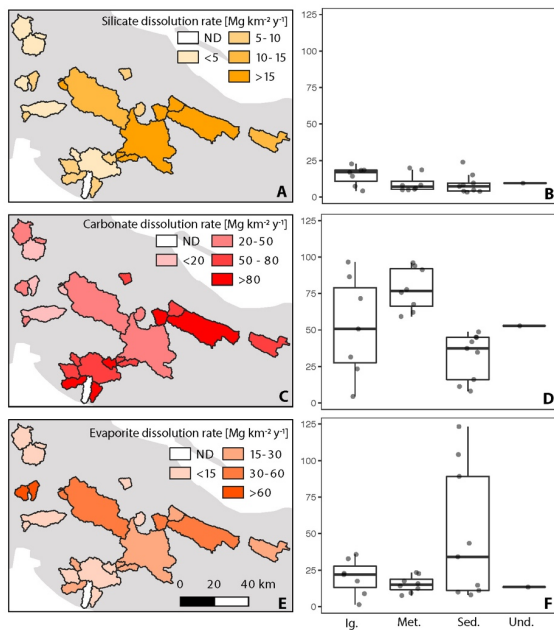


Figure 4: Dissolution rates partitioned by lithology. A,B. Silicate. C,D. Carbonate. E,F. Evaporite.
Darker colors represent higher rates. Box plots show the maximum and minimum values in the lines

extending from the box; the upper side of the box represents the upper quartile, the line inside of the box represents the median value, and the bottom of the box represents the lower quartile.

500

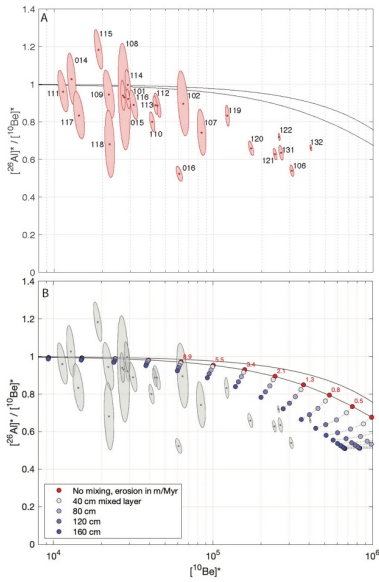


Figure 5: $^{26}\text{Al}/^{10}\text{Be}$ two-isotope plots. To permit comparison of data from different locations and elevations on the same plot, nuclide concentrations have been normalized by dividing measured concentrations by calculated mean production rates in the respective drainage basins, using production rate calculations from version 3 of the online exposure age calculator described by Balco et al. (2008) and subsequently updated. In both plots, uncertainty ellipses denote 68% confidence regions for the normalized nuclide concentrations, and the black lines are the boundaries of the simple exposure region (Lal, 1991) calculated using the conventional assumption of steady block erosion without vertical mixing. Panel A shows that $^{26}\text{Al}/^{10}\text{Be}$ ratios from basins with high nuclide concentrations, implying low erosion rates, are systematically lower than predicted by steady erosion without vertical mixing. Panel B shows that this inconsistency can, at least in part, be explained by the presence of a mixed layer of at least 160 cm. Circles show expected steady-state nuclide concentrations in a fully mixed surface layer calculated according to Lal and Chen (2005) for a range of erosion rates and mixed-layer thicknesses,

505

510

Two zoomed-in plots of the $^{26}\text{Al}/^{10}\text{Be}$ data from Figure 5. The top plot shows data points with uncertainty ellipses and a black line. The bottom plot shows data points with uncertainty ellipses and a black line, with a legend indicating different erosion rates and mixed layer thicknesses.

- Deleted:
- Formatted: Font: Bold
- Formatted: Don't adjust right indent when grid is defined, Line spacing: 1.5 lines, Don't snap to grid
- Formatted: Font: 12 pt, Not Bold
- Formatted: Don't adjust right indent when grid is defined, Don't snap to grid
- Deleted: 4:
- Formatted: Font: 12 pt, Not Bold
- Deleted: (leaving aside an anomalous result from CU-016)
- Formatted: Font: 12 pt, Not Bold
- Deleted: .
- Formatted: Font: 12 pt, Not Bold

which highlights that sediment derived from a deep mixed layer has lower nuclide concentrations and lower $^{26}\text{Al}/^{10}\text{Be}$ ratios than would be expected if the mixed layer were absent. Sample ID as in panel A.

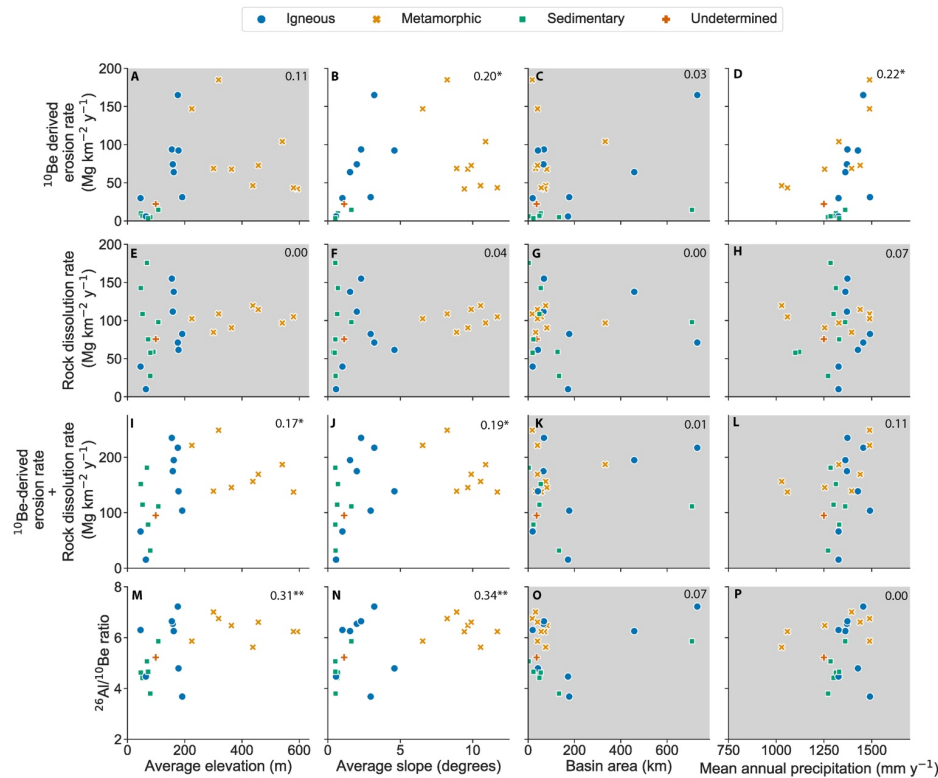
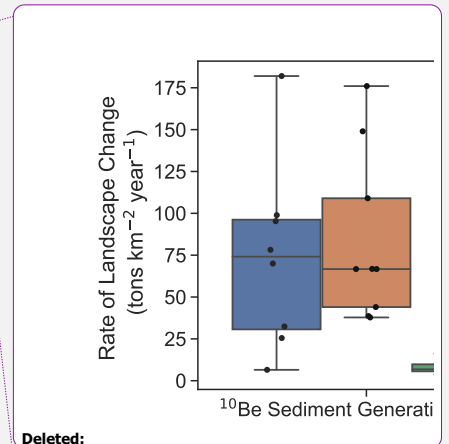


Figure 6. Relationship between measured ^{10}Be -derived erosion rates, chemical denudation rates, and the sum of chemical denudation rates and ^{10}Be -derived erosion rates to basin characteristics. Different shaped/colored points represent the dominant underlying rock type in that basin. Plots with $p > 0.05$ are shown with a gray background. Small numbers in upper right are R^2 values; * indicates $p \leq 0.05$, ** $p \leq 0.01$.



Deleted:

Formatted: Don't adjust right indent when grid is defined, Line spacing: 1.5 lines, Don't snap to grid

Deleted: Figure 5: Sediment generation rates and rock dissolution rates, classified by rock type. Box plots show the maximum and minimum values in the lines extending from the box; the upper side of the box represents the upper quartile, the line inside of the box represents the median value, and the bottom of the box represents the lower quartile. [163]

Formatted: Font: 12 pt, Not Bold

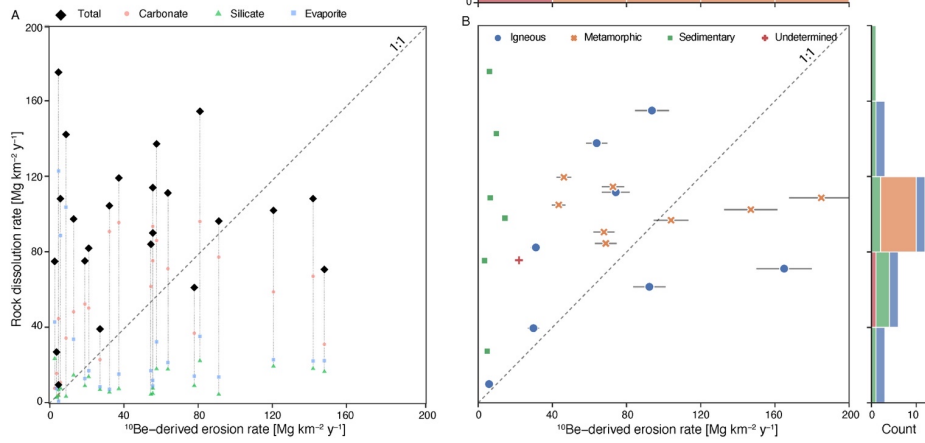
Deleted: 6:

Formatted: Font: 12 pt, Not Bold

Deleted: 1

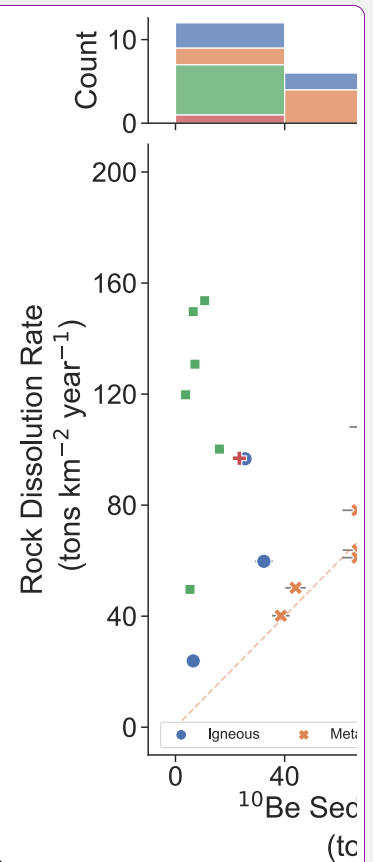
Formatted: Font: 12 pt, Not Bold

Formatted: Font: 12 pt, Not Bold



550 **Figure 7.** Scatterplot of rock dissolution rates vs. ^{10}Be -derived erosion rates. **A.** Data shown for
calculations of carbonate, silicate, and evaporite dissolution rates. **B.** Data shown for dominant
lithologies underlying each sampled basin. Horizontal lines extending from the points demonstrate the
uncertainty associated with the calculation of ^{10}Be -derived erosion rates. Histograms on axes show
distribution of data. **Dashed line is 1:1.**

555



- Deleted:**
- Formatted:** Font: 12 pt, Not Bold
- Deleted:** 7:
- Formatted:** Font: 12 pt, Not Bold
- Deleted:** sediment generation
- Formatted:** Don't adjust right indent when grid is defined, Line spacing: 1.5 lines, Don't snap to grid
- Formatted:** Font: 12 pt, Not Bold
- Deleted:** Dashed orange line is a 1:1 line.
- Formatted:** Font: 12 pt, Not Bold
- Deleted:** sediment generation
- Formatted:**

TABLE 1. Summary of Central Cuban Drainage Basin Data

Sample	Lithology	Latitude	Longitude	Slope	Area	MAP	10Be Erosion rate	±%	26Al Erosion rate	±%	26Al/10Be	±%	Total Disol	disol/10Be erosion	max rate
		(°N)	(°W)	(°)	(km ²)	(mm yr ⁻¹)	(Mg km ⁻² y ⁻¹)		(Mg km ⁻² y ⁻¹)				(Mg km ⁻² y ⁻¹)		(10Be+ disol)
CU-014	Igneous	22.0662	-79.7962	3.2	730	1456	163.0	14.6	161.0	21.2	7.15	0.64	71.2	0.44	234.2
CU-015	Igneous	22.1485	-79.4231	1.5	458	1362	64.5	5.7	71.4	8.3	6.32	0.38	137.7	2.13	202.2
CU-016	Igneous	22.2090	-78.0172	3.0	177	1491	31.2	2.7	61.6	7.1	3.69	0.19	82.4	2.64	113.6
CU-101	Metamorphic	22.0526	-80.2922	9.7	81	1254	67.7	5.6	73.0	8.2	6.46	0.27	90.5	1.34	158.2
CU-102	Sedimentary	22.3011	-80.5004	1.0	19	1327	30.3	3.0	32.2	5.3	6.41	0.84	39.6	1.31	69.9
CU-104	Sedimentary						ND	ND	ND	ND	ND	ND	58.9	ND	ND
CU-106	Sedimentary	22.7068	-80.3667	0.5	133	1272	4.8	0.5	9.0	1.2	3.80	0.15	27.4	5.65	32.2
CU-107	Undetermined	22.5354	-79.8796	1.1	37	1250	22.3	2.1	29.2	4.6	5.30	0.60	75.7	3.39	98.0
CU-108	Igneous	22.3924	-79.6691	2.0	66	1370	76.5	7.7	79.0	18.5	6.74	1.44	111.7	1.46	188.2
CU-109	Igneous	22.3570	-79.7612	2.3	68	1373	96.1	9.3	98.5	12.9	6.81	0.64	155.0	1.61	251.1
CU-110	Metamorphic	21.9187	-80.2659	10.5	76	1029	46.6	4.0	57.5	6.5	5.66	0.26	119.6	2.57	166.2
CU-111	Metamorphic	22.0895	-79.9169	8.2	17	1489	189.0	17.7	193.0	23.4	6.91	0.54	108.7	0.58	297.7
CU-112	Metamorphic	21.8326	-80.1503	9.4	71	1059	42.0	3.7	46.4	5.3	6.26	0.31	ND	ND	#VALUE!
CU-113	Metamorphic	21.8376	-80.1045	11.7	56	1059	43.3	3.6	48.3	5.4	6.23	0.24	104.9	2.42	146.2
CU-114	Metamorphic	22.1056	-80.2253	8.9	32	1395	68.3	5.8	67.9	7.9	6.99	0.38	84.5	1.24	152.8
CU-115	Metamorphic	22.1106	-80.1291	10.9	333	1328	106.0	9.4	86.5	9.9	8.42	0.50	96.8	0.91	202.8
CU-116	Metamorphic	22.0277	-79.9889	9.9	40	1440	72.4	6.0	76.6	9.2	6.59	0.39	114.6	1.58	187.0
CU-117	Metamorphic	22.0494	-79.8431	6.5	40	1489	145.0	14.1	178.0	24.8	5.80	0.62	102.4	0.71	247.4
CU-118	Igneous	22.3751	-79.8175	4.6	42	1428	94.3	8.8	139.0	28.9	4.89	0.90	61.5	0.65	155.8
CU-119	Sedimentary	22.5668	-80.2220	1.6	707	1361	14.5	1.2	16.6	2.0	5.87	0.27	97.9	6.75	112.4
CU-120	Sedimentary	22.4431	-80.4809	0.7	54	1313	9.8	0.9	14.7	1.8	4.63	0.18	142.7	14.58	152.5
CU-121	Sedimentary	22.4442	-80.4448	0.6	49	1300	6.5	0.6	10.1	1.3	4.42	0.15	108.7	16.69	115.2
CU-122	Sedimentary	22.5047	-80.2907	0.5	2	1285	6.0	4.9	7.9	1.0	5.06	3.58	175.7	29.08	181.7
CU-124	Sedimentary						ND	ND	ND	ND	ND	ND	57.8	ND	ND
CU-131	Igneous	22.3547	-80.5088	0.6	172	1326	5.9	0.5	9.0	1.2	4.48	0.19	10.0	1.70	15.8
CU-132	Sedimentary	22.4918	-80.2963	0.5	23	1329	3.4	3.0	4.8	0.7	4.65	3.29	75.4	22.12	78.8

ND = no data

10Be-derived erosion	Ratio of rock dissolution to 10Be-derived erosion	26Al/10Be ratio	Quartz yield	Carbonate dissolution rate	Silicate dissolution rate	Evaporite dissolution rate	Sum of rock dissolution and 10Be-derived erosion rate	Mean basin slope	Total basin area	Mean annual precipitation	% Agricultural land	Mean basin elevation	
0.12	0.36	0.25	0.32	0.59	0.32	0.65	0.65	0.19	-0.05	0.07	-0.27	0.22	Rock dissolution rate
	-0.55	0.64	-0.01	0.41	0.42	-0.32	0.83	0.44	0.18	0.47	-0.34	0.34	10Be-derived erosion
		-0.46	0.45	-0.43	-0.02	0.85	-0.22	-0.47	-0.20	-0.18	0.16	-0.45	Ratio of rock dissolution to 10Be-derived erosion
			0.17	0.60	0.14	-0.29	0.64	0.58	0.26	0.05	-0.49	0.56	26Al/10Be ratio
			0.13	-0.11	0.32	0.17	0.39	-0.19	-0.12	-0.61	0.33		Quartz yield
				0.16	-0.22	0.64	0.68	-0.02	-0.10	-0.54	0.74		Carbonate dissolution rate
					0.04	0.46	-0.13	0.23	0.52	0.24	-0.12		Silicate dissolution rate
						0.11	-0.36	-0.09	0.07	0.10	-0.38		Evaporite dissolution rate
							0.44	0.09	0.33	-0.40	0.41		Sum of rock dissolution and 10Be-derived erosion rate
								-0.11	-0.14	-0.79	0.95		Mean basin slope
									0.23	0.02	-0.05		Total basin area
										0.09	-0.27		Mean annual precipitation
											-0.74		% Agricultural land

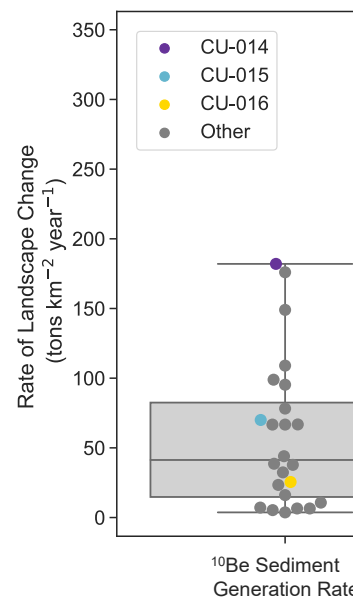
TABLE 2B. P-values for Linear Regressions

10Be-derived erosion	Ratio of rock dissolution to 10Be-derived erosion	26Al/10Be ratio	Quartz yield	Carbonate dissolution rate	Silicate dissolution rate	Evaporite dissolution rate	Sum of rock dissolution and 10Be-derived erosion rate	Mean basin slope	Total basin area	Mean annual precipitation	% Agricultural land	Mean basin elevation	
0.583	0.090	0.260	0.147	0.002	0.124	0.000	0.001	0.363	0.816	0.753	0.184	0.296	Rock dissolution rate
	0.006	0.001	0.977	0.054	0.047	0.143	0.000	0.029	0.397	0.020	0.113	0.105	10Be-derived erosion
		0.028	0.034	0.039	0.941	0.000	0.315	0.024	0.369	0.421	0.467	0.031	Ratio of rock dissolution to 10Be-derived erosion
			0.443	0.002	0.530	0.184	0.001	0.003	0.222	0.818	0.017	0.004	26Al/10Be ratio
				0.563	0.629	0.141	0.442	0.064	0.393	0.581	0.002	0.118	Quartz yield
					0.456	0.291	0.001	0.000	0.941	0.626	0.006	0.000	Carbonate dissolution rate
						0.848	0.025	0.540	0.279	0.007	0.248	0.571	Silicate dissolution rate
							0.605	0.076	0.653	0.754	0.636	0.062	Evaporite dissolution rate
								0.037	0.683	0.120	0.056	0.051	Sum of rock dissolution and 10Be-derived erosion rate
									0.596	0.501	0.000	0.000	Mean basin slope
										0.265	0.936	0.817	Total basin area
	p<0.01												Mean annual precipitation
		p<0.05									0.679	0.175	% Agricultural land
												0.000	

References

Reference List

- 575 Anderson, S. P., Blanckenburg, F. v., and White, A. F.: Physical and Chemical Controls on the Critical Zone, *Elements*, 3, 315-319, 2007.
- Balco, G. and Shuster, D. L.: Production rate of cosmogenic ^{21}Ne in quartz estimated from ^{10}Be , ^{26}Al , and ^{21}Ne concentrations in slowly eroding Antarctic bedrock surfaces, *Earth and Planetary Science Letters*, 281, 48-58, 10.1016/j.epsl.2009.02.006, 2009.
- Balco, G., Stone, J. O., Lifton, N. A., and Dunai, T. J.: A complete and easily accessible means of calculating surface exposure ages or erosion rates from ^{10}Be and ^{26}Al measurements, *Quaternary Geochronology*, 3, 174-195, 10.1016/j.quageo.2007.12.001, 2008.
- 580 Balter-Kennedy, A., Bromley, G., Balco, G., Thomas, H., and Jackson, M. S.: A 14.5-million-year record of East Antarctic Ice Sheet fluctuations from the central Transantarctic Mountains, constrained with cosmogenic ^{3}He , ^{10}Be , ^{21}Ne , and ^{26}Al , *The Cryosphere*, 14, 2647-2672, 10.5194/tc-14-2647-2020, 2020.
- Barreto, H. N., Varajão, C. A. C., Braucher, R., Bourlès, D. L., Salgado, A. A. R., and Varajão, A. F. D. C.: Denudation rates of the Southern Espinhaço Range, Minas Gerais, Brazil, determined by in situ-produced cosmogenic beryllium-10, *Geomorphology*, 191, 1-13, 10.1016/j.geomorph.2013.01.021, 2013.
- 585 Beck, H. E., de Roo, A., and van Dijk, A. I. J. M.: Global Maps of Streamflow Characteristics Based on Observations from Several Thousand Catchments*, *Journal of Hydrometeorology*, 16, 1478-1501, 10.1175/jhm-d-14-0155.1, 2015.
- Beck, H. E., Vergopolan, N., Pan, M., Levizzani, V., van Dijk, A. I. J. M., Weedon, G. P., Brocca, L., Pappenberger, F., Huffman, G. J., and Wood, E. F.: Global-scale evaluation of 22 precipitation datasets using gauge observations and hydrological modeling, *Hydrology and Earth System Sciences*, 21, 6201-6217, 10.5194/hess-21-6201-2017, 2017.
- 590 Bennett, H. H. and Allison, R. V.: *The soils of Cuba*, Tropical Plant Research Foundation, Washington, D.C.1928.
- Betancourt, C., Suárez, R., and Jorge, F.: Influencia de los procesos naturales y antrópicos sobre la calidad del agua en cuatro embalses cubanos, *Limnetica*, 31, 193-204, 2012.
- 595 Bierman, P. and Steig, E.: Estimating rates of denudation using cosmogenic isotope abundances in sediment, *Earth Surface Processes and Landforms*, 21, 103-203, 1996.
- Bierman, P., Herdandez, R. S., Schmidt, A., Aguila, H. C., Alvarez, Y., Arruebarrena, A., Campbell, M. K., Dethier, D., Dix, M., Massey-Bierman, M., Moya, A. G., Perdrill, J., Racela, J., and Alonso-Hernandez, C.: ¡Cuba! River Water Chemistry Reveals Rapid Chemical Weathering, the Echo of Uplift, and the Promise of More Sustainable Agriculture, *GSA Today*, 30, 4-10, 2020.
- 600 Bierman, P. R., Marsella, K. A., Patterson, C., Davis, P. T., & Caffee, M.: Mid-Pleistocene cosmogenic minimum-age limits for pre-Wisconsinan glacial surfaces in southwestern Minnesota and southern Baffin Island: a multiple nuclide approach, *Geomorphology*, 27, 27-39, 1999.
- Brown, E. T., Stallard, R. F., Larsen, M. C., Raisbeck, G. M., and Yiou, F.: Denudation rates determined from the accumulation of in situ-produced ^{10}Be in the Luquillo Experimental Forest, Puerto Rico, *Earth and Planetary Science Letters*, 129, 193-202, 1995.
- 605 Chapela Lara, M., Buss, H. L., Pogge von Strandmann, P. A. E., Schuessler, J. A., and Moore, O. W.: The influence of critical zone processes on the Mg isotope budget in a tropical, highly weathered andesitic catchment, *Geochimica et Cosmochimica Acta*, 202, 77-100, 10.1016/j.gca.2016.12.032, 2017.
- Cherem, L. F. S., Varajão, C. A. C., Braucher, R., Bourlès, D., Salgado, A. A. R., and Varajão, A. C.: Long-term evolution of denudational escarpments in southeastern Brazil, *Geomorphology*, 173-174, 118-127, 10.1016/j.geomorph.2012.06.002, 2012.
- 610 Codilean, A. T., Munack, H., Cohen, T. J., Saktura, W. M., Gray, A., and Mudd, S. M.: OCTOPUS: An Open Cosmogenic Isotope and Luminescence Database, *Earth System Science Data*, 10.5194/essd-2018-32, 2018.
- Corbett, L. B., Bierman, P. R., and Rood, D. H.: An approach for optimizing in situ cosmogenic ^{10}Be sample preparation, *Quaternary Geochronology*, 33, 24-34, 10.1016/j.quageo.2016.02.001, 2016.
- 615 Corbett, L. B., Bierman, P. R., Woodruff, T. E., and Caffee, M. W.: A homogeneous liquid reference material for monitoring the quality and reproducibility of in situ cosmogenic ^{10}Be and ^{26}Al analyses, *Nuclear Instruments and Methods in Physics Research Section B: Beam Interactions with Materials and Atoms*, 456, 180-185, 10.1016/j.nimb.2019.05.051, 2019.
- Derrieux, F., Siame, L. L., Bourlès, D. L., Chen, R.-F., Braucher, R., Léanni, L., Lee, J.-C., Chu, H.-T., and Byrne, T. B.: How fast is the denudation of the Taiwan mountain belt? Perspectives from in situ cosmogenic ^{10}Be , *Journal of Asian Earth Sciences*, 88, 230-245, 10.1016/j.jseas.2014.03.012, 2014.
- 620 Dixon, J. L., Heimsath, A. M., and Amundson, R.: The critical role of climate and saprolite weathering in landscape evolution, *Earth Surface Processes and Landforms*, 34, 1507-1521, 10.1002/esp.1836, 2009a.
- Dixon, J. L., Heimsath, A. M., Kaste, J., and Amundson, R.: Climate-driven processes of hillslope weathering, *Geology*, 37, 975-978, 10.1130/g30045a.1, 2009b.
- Dunne, T.: Rates of chemical denudation of silicate rocks in tropical catchments, *Nature*, 274, 244-246, 1978.



Deleted: Figure 8: Boxplots comparing long-term sediment generation rates measured in this study ($n = 24$) and erosion rates calculated using modern sediment yield data from island-wide observations ($n = 32$). Box plots show the maximum and minimum values in the lines extending from the box; the upper side of the box represents the upper quartile, the line inside of the box represents the median value, and the bottom of the box represents the lower quartile. Basins with both measurements are shown as colored points. Sediment yield data are from Pérez Zorrilla and Ya Karasik (1989) and represent points across the island of Cuba.

Formatted: Don't adjust right indent when grid is defined, Line spacing: 1.5 lines, Don't snap to grid

Formatted: Font: 12 pt

- Ferrier, K. L. and Kirchner, J. W.: Effects of physical erosion on chemical denudation rates: A numerical modeling study of soil-mantled hillslopes, *Earth and Planetary Science Letters*, 272, 591-599, 10.1016/j.epsl.2008.05.024, 2008.
- 640 French, C. D. and Schenk, C. J.: Map showing geology, oil and gas fields, and geologic provinces of the Caribbean Region: U.S. Geological Survey Open-File Report 97-470-K, 2004.
- Galford, G. L., Fernandez, M., Roman, J., Monasterolo, I., Ahamed, S., Fiske, G., González, P., and Kaufman, L.: Cuban land use and conservation, from rainforests to coral reefs, *Bulletin of Marine Science*, 10.5343/bms.2017.1026, 2018.
- Granger, D. E.: A review of burial dating methods using ²⁶Al and ¹⁰Be, in: *In-Situ Produced Cosmogenic Nuclides and Quantification of Geological Processes*, edited by: Siame, L. L., Bourlès, D. L., and Brown, E. T., The Geological Society of America, 1-16, 2006.
- 645 Granger, D. E. and Muzikar, P.: Dating sediment burial with in situ-produced cosmogenic nuclides: theory, techniques, and limitations, *Earth and Planetary Science Letters*, 188, 269-281, 2001.
- Granger, D. E., Kirchner, J. W., and Finkel, R.: Spatially Averaged Long-Term Erosion Rates Measured from In Situ-Produced Cosmogenic Nuclides in Alluvial Sediment, *The Journal of Geology*, 104, 249-257, 1996.
- 650 Hijmans, R. J., Cameron, S. E., Parra, J. L., Jones, P. G., and Jarvis, A.: Very high resolution interpolated climate surfaces for global land areas, *International Journal of Climatology*, 25, 1965-1978, 10.1002/joc.1276, 2005.
- Hinderer, M., Pflanz, D., and Schneider, S.: Chemical Denudation Rates in the Humid Tropics of East Africa and Comparison with ¹⁰Be-Derived Erosion Rates, *Procedia Earth and Planetary Science*, 7, 360-364, 10.1016/j.proeps.2013.03.047, 2013.
- Hu, X., Kirby, E., Pan, B., Granger, D. E., and Su, H.: Cosmogenic burial ages reveal sediment reservoir dynamics along the Yellow River, *China, Geology*, 39, 839-842, 10.1130/g32030.1, 2011.
- 655 Iturralde-Vinent, M. A., García-Casco, A., Rojas-Agramonte, Y., Proenza, J. A., Murphy, J. B., and Stern, R. J.: The geology of Cuba: A brief overview and synthesis, *GSA Today*, 4-10, 10.1130/gsatg296a.1, 2016.
- Jonell, T. N., Clift, P. D., Hoang, L. V., Hoang, T., Carter, A., Wittmann, H., Böning, P., Pahnke, K., and Rittenour, T.: Controls on erosion patterns and sediment transport in a monsoonal, tectonically quiescent drainage, Song Gianh, central Vietnam, *Basin Research*, 29, 659-683, 10.1111/bre.12199, 2017.
- 660 Kirchner, J. W., Finkel, R. C., Riebe, C. S., Granger, D. E., Clayton, J. L., King, J. G., and Megahan, W. F.: Mountain erosion over 10 yr, 10 k.y., and 10 m.y. time scales, *Geology*, 29, 591-594, 2001.
- Klein, J., Giegengack, R., Middleton, R., Sharma, P., Underwood, J., and Weeks, R.: Revealing histories of exposure using in situ produced ²⁶Al and ¹⁰Be in Libyan Desert glass, *Radiocarbon*, 28, 547-555, 1986.
- 665 Kohl, C. P. and Nishiizumi, K.: Chemical isolation of quartz for measurement of in-situ -produced cosmogenic nuclides, *Geochimica et Cosmochimica Acta*, 56, 3583-3587, 1992.
- Kurtz, A. C., Lugolobi, F., and Salvucci, G.: Germanium-silicon as a flow path tracer: Application to the Rio Icaos watershed, *Water Resources Research*, 47, 10.1029/2010wr009853, 2011.
- Lal, D.: Cosmic ray labeling of erosion surfaces: in situ nuclide production rates and erosion models, *Earth and Planetary Science Letters*, 104, 424-439, 1991.
- 670 Lal, D. and Chen, J.: Cosmic ray labeling of erosion surfaces II: Special cases of exposure histories of boulders, soils and beach terraces, *Earth and Planetary Science Letters*, 236, 797-813, 10.1016/j.epsl.2005.05.025, 2005.
- Larsen, I. J., Montgomery, D. R., and Greenberg, H. M.: The contribution of mountains to global denudation, *Geology*, 42, 527-530, 10.1130/g35136.1, 2014.
- 675 Llacer, I. D.: Comportamiento de la precipitación en estaciones meteorológicas seleccionadas de Cuba, Facultad de Geografía, La Universidad de la Habana, La Habana, Cuba, 2012.
- LPDAAC: ASTER GDEM (Volume 2019) [dataset],
- Lukens, C. E., Riebe, C. S., Sklar, L. S., and Shuster, D. L.: Grain size bias in cosmogenic nuclide studies of stream sediment in steep terrain, *Journal of Geophysical Research: Earth Surface*, 121, 978-999, 10.1002/2016jfr003859, 2016.
- 680 Makhubela, T. V., Kramers, J. D., Scherler, D., Wittmann, H., Dirks, P. H. G. M., and Winkler, S. R.: Effects of long soil surface residence times on apparent cosmogenic nuclide denudation rates and burial ages in the Cradle of Humankind, South Africa, *Earth Surface Processes and Landforms*, 44, 2968-2981, 10.1002/esp.4723, 2019.
- Mandal, S. K., Lupker, M., Burg, J.-P., Valla, P. G., Haghipour, N., and Christl, M.: Spatial variability of ¹⁰Be-derived erosion rates across the southern Peninsular Indian escarpment: A key to landscape evolution across passive margins, *Earth and Planetary Science Letters*, 425, 154-167, 10.1016/j.epsl.2015.05.050, 2015.
- 685 Marshall, J. A., Roering, J. J., Gavin, D. G., and Granger, D. E.: Late Quaternary climatic controls on erosion rates and geomorphic processes in western Oregon, USA, *Geological Society of America Bulletin*, 129, 715-731, 10.1130/b31509.1, 2017.
- Modenesi-Gauttieri, M. C., de Toledo, M. C. M., Hiruma, S. T., Taioli, F., and Shimada, H.: Deep weathering and landscape evolution in a tropical plateau, *Catena*, 85, 221-230, 10.1016/j.catena.2011.01.006, 2011.
- 690 Moore, O. W., Buss, H. L., and Dosseto, A.: Incipient chemical weathering at bedrock fracture interfaces in a tropical critical zone system, Puerto Rico, *Geochimica et Cosmochimica Acta*, 252, 61-87, 10.1016/j.gca.2019.02.028, 2019.
- Nearing, M. A., Xie, Y., Liu, B., and Ye, Y.: Natural and anthropogenic rates of soil erosion, *International Soil and Water Conservation Research*, 5, 77-84, 10.1016/j.iswcr.2017.04.001, 2017.

- 695 Nishiizumi, K.: Preparation of ²⁶Al AMS standards, *Nuclear Instruments and Methods in Physics Research Section B: Beam Interactions with Materials and Atoms*, 223-224, 388-392, <https://doi.org/10.1016/j.nimb.2004.04.075>, 2004.
- Nishiizumi, K., Imamura, M., Caffee, M. W., Southon, J. R., Finkel, R. C., and McAninch, J.: Absolute calibration of ¹⁰Be AMS standards, *Nuclear Instruments and Methods in Physics Research Section B: Beam Interactions with Materials and Atoms*, 258, 403-413, 10.1016/j.nimb.2007.01.297, 2007.
- 700 Nishiizumi, K., Winterer, E. L., Kohl, C. P., Klein, J., Middleton, R., Lal, D., and Arnold, J. R.: Cosmic ray production rates of ¹⁰Be and ²⁶Al in quartz from glacially polished rocks, *Journal of Geophysical Research*, 94, 10.1029/JB094iB12p17907, 1989.
- Ollier, C. D.: Deep Weathering, Groundwater and Climate, *Geografiska Annaler*, 70, 285- 290, 1988.
- Pardo, G.: *Geology of Cuba*. AAPG Studies in Geology, The American Association of Petroleum Geologists, Tulsa, Oklahoma 2009.
- Pérez Zorrilla, W. and Ya Karasik, G.: El escurrimiento solido y la erosión hidrica actual de Cuba, *Ciencias de la tierra y del espacio*, 15-16, 67-76, 1989.
- 705 Pope, G. A.: Weathering in the tropics, and related extratropical processes, in: *Treatise on Geomorphology*, edited by: Shroder, J., Weathering and Soils Geomorphology, Academic Press, 2013.
- Portenga, E. W. and Bierman, P. R.: Understanding Earth's eroding surface with ¹⁰Be, *GSA Today*, 21, 4-10, 10.1130/g111a.1, 2011.
- Préndez, M., López, R., and Carrillo, E.: Physical and Chemical Components of Cuba's Rain: Effects on Air Quality, *International Journal of Atmospheric Sciences*, 2014, 1-8, 10.1155/2014/680735, 2014.
- 710 Pulina, M. and Fagundo, J. R.: Tropical karst and chemical denudation of western Cuba, *Geographia Polonica*, 60, 195-216, 1992.
- Rad, S., Allegre, C., and Louvat, P.: Hidden erosion on volcanic islands, *Earth and Planetary Science Letters*, 262, 109-124, 10.1016/j.epsl.2007.07.019, 2007.
- Rad, S., Rivé, K., Vittecoq, B., Cerdan, O., and Allègre, C. J.: Chemical weathering and erosion rates in the Lesser Antilles: An overview in Guadeloupe, Martinique and Dominica, *Journal of South American Earth Sciences*, 45, 331-344, 10.1016/j.jsames.2013.03.004, 2013.
- 715 Regard, V., Carretier, S., Boeglin, J.-L., Ndam Ngoupayou, J.-R., Dzana, J.-G., Bedimo Bedimo, J.-P., Riotte, J., and Braun, J.-J.: Denudation rates on cratonic landscapes: comparison between suspended and dissolved fluxes, and ¹⁰Be analysis in the Nyong and Sanaga River basins, south Cameroon, *Earth Surface Processes and Landforms*, 41, 1671-1683, 10.1002/esp.3939, 2016.
- Reinhardt, L. J., Bishop, P., Hoey, T. B., Dempster, T. J., and Sanderson, D. C. W.: Quantification of the transient response to base-level fall in a small mountain catchment: Sierra Nevada, southern Spain, *Journal of Geophysical Research*, 112, 10.1029/2006j000524, 2007.
- 720 Reusser, L., Bierman, P., and Rood, D.: Quantifying human impacts on rates of erosion and sediment transport at a landscape scale, *Geology*, 43, 171-174, 2015.
- Riebe, C. S. and Granger, D. E.: Quantifying effects of deep and near-surface chemical erosion on cosmogenic nuclides in soils, saprolite, and sediment, *Earth Surface Processes and Landforms*, 38, 523-533, 10.1002/esp.3339, 2013.
- 725 Riebe, C. S., Kirchner, J. W., and Finkel, R. C.: Long-term rates of chemical weathering and physical erosion from cosmogenic nuclides and geochemical mass balance, *Geochimica et Cosmochimica Acta*, 67, 4411-4427, 10.1016/s0016-7037(03)00382-x, 2003.
- Riebe, C. S., Kirchner, J. W., and Granger, D. E.: Quantifying quartz enrichment and its consequences for cosmogenic measurements of erosion rates from alluvial sediment and regolith, *Geomorphology*, 15-19, 2001a.
- Riebe, C. S., Kirchner, J. W., Granger, D. E., and Finkel, R. C.: Minimal climatic control on erosion rates in the Sierra Nevada, California, *The Journal of Geology*, 29, 447-450, 2001b.
- 730 Salgado, A. A. R., Braucher, R., Colin, F., Nalini, H. A., Varajão, A. F. D. C., and Varajão, C. A. C.: Denudation rates of the Quadrilátero Ferrífero (Minas Gerais, Brazil): Preliminary results from measurements of solute fluxes in rivers and in situ-produced cosmogenic ¹⁰Be, *Journal of Geochemical Exploration*, 88, 313-317, 10.1016/j.gexplo.2005.08.064, 2006.
- Scherler, D., Bookhagen, B., and Strecker, M. R.: Tectonic control on ¹⁰Be-derived erosion rates in the Garhwal Himalaya, India, *Journal of Geophysical Research: Earth Surface*, 119, 83-105, 10.1002/2013j002955, 2014.
- 735 Schopka, H. H. and Derry, L. A.: Chemical weathering fluxes from volcanic islands and the importance of groundwater: The Hawaiian example, *Earth and Planetary Science Letters*, 339-340, 67-78, 10.1016/j.epsl.2012.05.028, 2012.
- Small, E. E., Anderson, R. S., and Hancock, G. S.: Estimates of the rate of regolith production using ¹⁰Be and ²⁶Al from an alpine hillslope, *Geomorphology*, 131-150, 1999.
- 740 Sosa Gonzalez, V., Bierman, P. R., Fernandes, N. F., and Rood, D. H.: Long-term background denudation rates of southern and southeastern Brazilian watersheds estimated with cosmogenic ¹⁰Be, *Geomorphology*, 268, 54-63, 10.1016/j.geomorph.2016.05.024, 2016a.
- Sosa Gonzalez, V., Bierman, P. R., Nichols, K. K., and Rood, D. H.: Long-term erosion rates of Panamanian drainage basins determined using in situ ¹⁰Be, *Geomorphology*, 275, 1-15, 10.1016/j.geomorph.2016.04.025, 2016b.
- 745 Stone, J. O.: Air pressure and cosmogenic isotope production, *Journal of Geophysical Research: Solid Earth*, 105, 23753-23759, 10.1029/2000jb900181, 2000.
- Struck, M., Jansen, J. D., Fujioka, T., Codilean, A. T., Fink, D., Egholm, D. L., Fülöp, R.-H., Wilcken, K. M., and Kotevski, S.: Soil production and transport on postorogenic desert hillslopes quantified with ¹⁰Be and ²⁶Al, *GSA Bulletin*, 130, 1017-1040, 10.1130/b31767.1, 2018.
- Vasconcelos, P. M., Farley, K. A., Stone, J., Piacentini, T., and Fifield, L. K.: Stranded landscapes in the humid tropics: Earth's oldest land surfaces, *Earth and Planetary Science Letters*, 519, 152-164, 10.1016/j.epsl.2019.04.014, 2019.

- 750 von Blanckenburg, F., Hewawasam, T., and Kubik, P. W.: Cosmogenic nuclide evidence for low weathering and denudation in the wet, tropical highlands of Sri Lanka, *Journal of Geophysical Research*, 109, 1-22, 10.1029/2003JF000049, 2004.
- West, A., Galy, A., and Bickle, M.: Tectonic and climatic controls on silicate weathering, *Earth and Planetary Science Letters*, 235, 211-228, 10.1016/j.epsl.2005.03.020, 2005.
- 755 Whitbeck, R. H.: Geographical Relations in the Development of Cuban Agriculture, *American Geographical Society*, 12, 223-240, 1922.
- White, A., Blum, A., Schulz, M., Vivit, D., Stonestrom, D., Larsen, M., Murphy, S., and Eberl, D.: Chemical weathering in a tropical watershed, Luquillo Mountains, Puerto Rico: I. Long-term versus short-term weathering fluxes, *Geochemica et Cosmochimica Acta*, 62, 209-226, 1998.
- White, A. F. and Blum, A. E.: Effects of climate on chemical weathering in watersheds, *Geochemica et Cosmochimica Acta*, 59, 1729-1747, 1995.
- 760 Wittmann, H., von Blanckenburg, F., Maurice, L., Guyot, J. L., and Kubik, P. W.: Recycling of Amazon floodplain sediment quantified by cosmogenic ^{26}Al and ^{10}Be , *Geology*, 39, 467-470, 10.1130/g31829.1, 2011.

Formatted: Font: 12 pt

Formatted: Don't adjust right indent when grid is defined, Line spacing: 1.5 lines, Don't snap to grid

765

Formatted: Font: 12 pt

Page 1: [1] Style Definition **Amanda Schmidt** **4/25/22 1:43:00 PM**

Comment Text: Font: 10 pt, English (UK), Justified

Page 1: [2] Style Definition **Amanda Schmidt** **4/25/22 1:43:00 PM**

EndNote Bibliography Title: Line spacing: 1.5 lines

Page 1: [3] Style Definition **Amanda Schmidt** **4/25/22 1:43:00 PM**

Correspondence: Font: 10 pt, English (UK), Justified

Page 1: [4] Style Definition **Amanda Schmidt** **4/25/22 1:43:00 PM**

Equation: Font: 10 pt, English (UK), Justified, Line spacing: 1.5 lines

Page 1: [5] Style Definition **Amanda Schmidt** **4/25/22 1:43:00 PM**

Affiliation: Font: 10 pt, English (UK), Justified

Page 1: [6] Style Definition **Amanda Schmidt** **4/25/22 1:43:00 PM**

List Paragraph: Font: 10 pt, English (UK), Justified, Line spacing: 1.5 lines

Page 1: [7] Style Definition **Amanda Schmidt** **4/25/22 1:43:00 PM**

Copernicus_Word_template: Font: 10 pt, English (UK), Justified, Line spacing: 1.5 lines

Page 1: [8] Style Definition **Amanda Schmidt** **4/25/22 1:43:00 PM**

Name: English (UK), Justified, Line spacing: 1.5 lines

Page 1: [9] Style Definition **Amanda Schmidt** **4/25/22 1:43:00 PM**

Header: Font: 10 pt, English (UK), Justified, Line spacing: 1.5 lines

Page 1: [10] Style Definition **Amanda Schmidt** **4/25/22 1:43:00 PM**

Bullets: Font: 10 pt, English (UK), Justified, Indent: Left: 0", First line: 0", Line spacing: 1.5 lines, Bulleted + Level: 1 + Aligned at: 0.25" + Indent at: 0.5", Tab stops: 0.25", List tab

Page 1: [11] Formatted **Amanda Schmidt** **4/25/22 1:43:00 PM**

Don't adjust right indent when grid is defined, Line spacing: 1.5 lines, Don't snap to grid

Page 1: [12] Formatted **Amanda Schmidt** **4/25/22 1:43:00 PM**

Don't adjust right indent when grid is defined, Line spacing: 1.5 lines, Don't snap to grid

Page 2: [13] Deleted **Amanda Schmidt** **4/25/22 1:43:00 PM**

▼

Page 2: [13] Deleted **Amanda Schmidt** **4/25/22 1:43:00 PM**

▼

Page 2: [13] Deleted **Amanda Schmidt** **4/25/22 1:43:00 PM**

▼

Page 2: [13] Deleted **Amanda Schmidt** **4/25/22 1:43:00 PM**

▼

Page 2: [13] Deleted **Amanda Schmidt** **4/25/22 1:43:00 PM**

▼

Page 2: [13] Deleted **Amanda Schmidt** **4/25/22 1:43:00 PM**



Page 2: [14] Formatted **Amanda Schmidt** **4/25/22 1:43:00 PM**

Font color: Text 1

Page 2: [14] Formatted **Amanda Schmidt** **4/25/22 1:43:00 PM**

Font color: Text 1

Page 2: [15] Formatted **Amanda Schmidt** **4/25/22 1:43:00 PM**

Font color: Text 1

Page 2: [16] Formatted **Amanda Schmidt** **4/25/22 1:43:00 PM**

Font color: Text 1

Page 2: [17] Formatted **Amanda Schmidt** **4/25/22 1:43:00 PM**

Font color: Text 1

Page 2: [18] Formatted **Amanda Schmidt** **4/25/22 1:43:00 PM**

Font color: Text 1

Page 2: [19] Formatted **Amanda Schmidt** **4/25/22 1:43:00 PM**

Font color: Text 1

Page 2: [20] Formatted **Amanda Schmidt** **4/25/22 1:43:00 PM**

Font color: Text 1

Page 2: [21] Formatted **Amanda Schmidt** **4/25/22 1:43:00 PM**

Font color: Text 1

Page 2: [22] Formatted **Amanda Schmidt** **4/25/22 1:43:00 PM**

Font color: Text 1

Page 2: [23] Formatted **Amanda Schmidt** **4/25/22 1:43:00 PM**

Font color: Text 1

Page 2: [24] Formatted **Amanda Schmidt** **4/25/22 1:43:00 PM**

Font color: Text 1

Page 2: [25] Formatted **Amanda Schmidt** **4/25/22 1:43:00 PM**

Font color: Text 1

Page 2: [26] Formatted **Amanda Schmidt** **4/25/22 1:43:00 PM**

Font color: Text 1

Page 2: [27] Deleted **Amanda Schmidt** **4/25/22 1:43:00 PM**



Page 2: [27] Deleted **Amanda Schmidt** **4/25/22 1:43:00 PM**



Page 2: [28] Formatted **Amanda Schmidt** **4/25/22 1:43:00 PM**

▼

Page 2: [30] Formatted	Amanda Schmidt	4/25/22 1:43:00 PM
-------------------------------	-----------------------	---------------------------

Font color: Text 1

Page 2: [31] Formatted	Amanda Schmidt	4/25/22 1:43:00 PM
-------------------------------	-----------------------	---------------------------

Font color: Text 1

Page 2: [32] Formatted	Amanda Schmidt	4/25/22 1:43:00 PM
-------------------------------	-----------------------	---------------------------

Font color: Text 1

Page 2: [33] Formatted	Amanda Schmidt	4/25/22 1:43:00 PM
-------------------------------	-----------------------	---------------------------

Font color: Text 1

Page 2: [34] Formatted	Amanda Schmidt	4/25/22 1:43:00 PM
-------------------------------	-----------------------	---------------------------

Font color: Text 1

Page 2: [35] Formatted	Amanda Schmidt	4/25/22 1:43:00 PM
-------------------------------	-----------------------	---------------------------

Indent: First line: 0.5", Don't adjust right indent when grid is defined, Line spacing: 1.5 lines, Don't snap to grid

Page 2: [36] Formatted	Amanda Schmidt	4/25/22 1:43:00 PM
-------------------------------	-----------------------	---------------------------

Font color: Text 1

Page 2: [37] Formatted	Amanda Schmidt	4/25/22 1:43:00 PM
-------------------------------	-----------------------	---------------------------

Font color: Text 1

Page 2: [38] Formatted	Amanda Schmidt	4/25/22 1:43:00 PM
-------------------------------	-----------------------	---------------------------

Font color: Text 1

Page 2: [39] Deleted	Amanda Schmidt	4/25/22 1:43:00 PM
-----------------------------	-----------------------	---------------------------

▼

Page 2: [40] Formatted	Amanda Schmidt	4/25/22 1:43:00 PM
-------------------------------	-----------------------	---------------------------

Font color: Text 1

Page 2: [40] Formatted	Amanda Schmidt	4/25/22 1:43:00 PM
-------------------------------	-----------------------	---------------------------

Font color: Text 1

Page 2: [41] Deleted	Amanda Schmidt	4/25/22 1:43:00 PM
-----------------------------	-----------------------	---------------------------

▼

Page 2: [42] Formatted	Amanda Schmidt	4/25/22 1:43:00 PM
-------------------------------	-----------------------	---------------------------

Font color: Text 1

Page 2: [43] Formatted	Amanda Schmidt	4/25/22 1:43:00 PM
-------------------------------	-----------------------	---------------------------

Font: 12 pt

Page 2: [44] Formatted	Amanda Schmidt	4/25/22 1:43:00 PM
-------------------------------	-----------------------	---------------------------

Don't adjust right indent when grid is defined, Line spacing: 1.5 lines, Don't snap to grid

Page 2: [45] Deleted	Amanda Schmidt	4/25/22 1:43:00 PM
-----------------------------	-----------------------	---------------------------

▼
Page 3: [46] Deleted **Amanda Schmidt** **4/25/22 1:43:00 PM**

▼
Page 11: [47] Deleted **Amanda Schmidt** **4/25/22 1:43:00 PM**

▼
Page 11: [48] Deleted **Amanda Schmidt** **4/25/22 1:43:00 PM**

▼
Page 15: [49] Deleted **Amanda Schmidt** **4/25/22 1:43:00 PM**

▼
Page 16: [50] Formatted **Amanda Schmidt** **4/25/22 1:43:00 PM**

Font: 12 pt, Font color: Text 1

Page 16: [51] Formatted **Amanda Schmidt** **4/25/22 1:43:00 PM**

Don't adjust right indent when grid is defined, Line spacing: 1.5 lines, Don't snap to grid

Page 16: [52] Formatted **Amanda Schmidt** **4/25/22 1:43:00 PM**

Font: 12 pt, Font color: Text 1,

Page 16: [53] Formatted **Amanda Schmidt** **4/25/22 1:43:00 PM**

Line spacing: 1.5 lines

Page 16: [54] Formatted **Amanda Schmidt** **4/25/22 1:43:00 PM**

Font color: Text 1

Page 16: [55] Deleted **Amanda Schmidt** **4/25/22 1:43:00 PM**

▼
Page 16: [56] Formatted **Amanda Schmidt** **4/25/22 1:43:00 PM**

Font color: Text 1

Page 16: [57] Formatted **Amanda Schmidt** **4/25/22 1:43:00 PM**

Font color: Text 1

Page 16: [58] Formatted **Amanda Schmidt** **4/25/22 1:43:00 PM**

Font color: Text 1

Page 16: [58] Formatted **Amanda Schmidt** **4/25/22 1:43:00 PM**

Font color: Text 1

Page 16: [59] Deleted **Amanda Schmidt** **4/25/22 1:43:00 PM**

▼
Page 16: [60] Formatted **Amanda Schmidt** **4/25/22 1:43:00 PM**

Don't adjust right indent when grid is defined, Line spacing: 1.5 lines, Don't snap to grid

Page 16: [61] Formatted **Amanda Schmidt** **4/25/22 1:43:00 PM**

Font color: Text 1

Page 16: [62] Formatted **Amanda Schmidt** **4/25/22 1:43:00 PM**

Font color: Text 1

Page 16: [64] Formatted	Amanda Schmidt	4/25/22 1:43:00 PM
--------------------------------	-----------------------	---------------------------

Font color: Text 1

Page 16: [65] Formatted	Amanda Schmidt	4/25/22 1:43:00 PM
--------------------------------	-----------------------	---------------------------

Font color: Text 1

Page 16: [65] Formatted	Amanda Schmidt	4/25/22 1:43:00 PM
--------------------------------	-----------------------	---------------------------

Font color: Text 1

Page 16: [65] Formatted	Amanda Schmidt	4/25/22 1:43:00 PM
--------------------------------	-----------------------	---------------------------

Font color: Text 1

Page 16: [65] Formatted	Amanda Schmidt	4/25/22 1:43:00 PM
--------------------------------	-----------------------	---------------------------

Font color: Text 1

Page 16: [65] Formatted	Amanda Schmidt	4/25/22 1:43:00 PM
--------------------------------	-----------------------	---------------------------

Font color: Text 1

Page 16: [66] Formatted	Amanda Schmidt	4/25/22 1:43:00 PM
--------------------------------	-----------------------	---------------------------

Font color: Text 1

Page 16: [67] Formatted	Amanda Schmidt	4/25/22 1:43:00 PM
--------------------------------	-----------------------	---------------------------

Font color: Text 1

Page 16: [68] Formatted	Amanda Schmidt	4/25/22 1:43:00 PM
--------------------------------	-----------------------	---------------------------

Font color: Text 1

Page 16: [68] Formatted	Amanda Schmidt	4/25/22 1:43:00 PM
--------------------------------	-----------------------	---------------------------

Font color: Text 1

Page 16: [69] Formatted	Amanda Schmidt	4/25/22 1:43:00 PM
--------------------------------	-----------------------	---------------------------

Font color: Text 1

Page 16: [70] Formatted	Amanda Schmidt	4/25/22 1:43:00 PM
--------------------------------	-----------------------	---------------------------

Font color: Text 1

Page 16: [71] Formatted	Amanda Schmidt	4/25/22 1:43:00 PM
--------------------------------	-----------------------	---------------------------

Font color: Text 1

Page 16: [72] Formatted	Amanda Schmidt	4/25/22 1:43:00 PM
--------------------------------	-----------------------	---------------------------

Font color: Text 1

Page 16: [73] Formatted	Amanda Schmidt	4/25/22 1:43:00 PM
--------------------------------	-----------------------	---------------------------

Font color: Text 1

Page 16: [74] Formatted	Amanda Schmidt	4/25/22 1:43:00 PM
--------------------------------	-----------------------	---------------------------

Font color: Text 1

Page 16: [74] Formatted	Amanda Schmidt	4/25/22 1:43:00 PM
--------------------------------	-----------------------	---------------------------

Font color: Text 1

Page 16: [75] Formatted	Amanda Schmidt	4/25/22 1:43:00 PM
--------------------------------	-----------------------	---------------------------

Font color: Text 1

Page 16: [77] Formatted	Amanda Schmidt	4/25/22 1:43:00 PM
--------------------------------	-----------------------	---------------------------

Font color: Text 1

Page 16: [78] Formatted	Amanda Schmidt	4/25/22 1:43:00 PM
--------------------------------	-----------------------	---------------------------

Font color: Text 1

Page 16: [79] Formatted	Amanda Schmidt	4/25/22 1:43:00 PM
--------------------------------	-----------------------	---------------------------

Font color: Text 1

Page 16: [79] Formatted	Amanda Schmidt	4/25/22 1:43:00 PM
--------------------------------	-----------------------	---------------------------

Font color: Text 1

Page 16: [80] Formatted	Amanda Schmidt	4/25/22 1:43:00 PM
--------------------------------	-----------------------	---------------------------

Font color: Text 1

Page 16: [81] Formatted	Amanda Schmidt	4/25/22 1:43:00 PM
--------------------------------	-----------------------	---------------------------

Font color: Text 1

Page 16: [81] Formatted	Amanda Schmidt	4/25/22 1:43:00 PM
--------------------------------	-----------------------	---------------------------

Font color: Text 1

Page 16: [82] Formatted	Amanda Schmidt	4/25/22 1:43:00 PM
--------------------------------	-----------------------	---------------------------

Font color: Text 1

Page 17: [83] Deleted	Amanda Schmidt	4/25/22 1:43:00 PM
------------------------------	-----------------------	---------------------------

▼

Page 17: [84] Formatted	Amanda Schmidt	4/25/22 1:43:00 PM
--------------------------------	-----------------------	---------------------------

Don't adjust right indent when grid is defined, Line spacing: 1.5 lines, Don't snap to grid

Page 17: [85] Formatted	Amanda Schmidt	4/25/22 1:43:00 PM
--------------------------------	-----------------------	---------------------------

Indent: First line: 0.5", Don't adjust right indent when grid is defined, Line spacing: 1.5 lines, Don't snap to grid

Page 18: [86] Formatted	Amanda Schmidt	4/25/22 1:43:00 PM
--------------------------------	-----------------------	---------------------------

Font color: Text 1

Page 18: [86] Formatted	Amanda Schmidt	4/25/22 1:43:00 PM
--------------------------------	-----------------------	---------------------------

Font color: Text 1

Page 18: [87] Formatted	Amanda Schmidt	4/25/22 1:43:00 PM
--------------------------------	-----------------------	---------------------------

Font color: Text 1

Page 18: [88] Formatted	Amanda Schmidt	4/25/22 1:43:00 PM
--------------------------------	-----------------------	---------------------------

Font color: Text 1,

Page 18: [88] Formatted	Amanda Schmidt	4/25/22 1:43:00 PM
--------------------------------	-----------------------	---------------------------

Font color: Text 1,

Page 18: [88] Formatted	Amanda Schmidt	4/25/22 1:43:00 PM
--------------------------------	-----------------------	---------------------------

Font color: Text 1,

Page 18: [89] Formatted	Amanda Schmidt	4/25/22 1:43:00 PM
--------------------------------	-----------------------	---------------------------

Don't adjust right indent when grid is defined, Line spacing: 1.5 lines, Don't snap to grid

Page 18: [91] Formatted	Amanda Schmidt	4/25/22 1:43:00 PM
--------------------------------	-----------------------	---------------------------

Font color: Text 1

Page 18: [92] Deleted	Amanda Schmidt	4/25/22 1:43:00 PM
------------------------------	-----------------------	---------------------------

Page 18: [93] Formatted	Amanda Schmidt	4/25/22 1:43:00 PM
--------------------------------	-----------------------	---------------------------

Font color: Text 1

Page 18: [94] Formatted	Amanda Schmidt	4/25/22 1:43:00 PM
--------------------------------	-----------------------	---------------------------

Font color: Text 1

Page 18: [95] Formatted	Amanda Schmidt	4/25/22 1:43:00 PM
--------------------------------	-----------------------	---------------------------

Font color: Text 1

Page 18: [96] Formatted	Amanda Schmidt	4/25/22 1:43:00 PM
--------------------------------	-----------------------	---------------------------

Font color: Text 1

Page 18: [97] Formatted	Amanda Schmidt	4/25/22 1:43:00 PM
--------------------------------	-----------------------	---------------------------

Font color: Text 1

Page 18: [98] Formatted	Amanda Schmidt	4/25/22 1:43:00 PM
--------------------------------	-----------------------	---------------------------

Font color: Text 1

Page 18: [99] Formatted	Amanda Schmidt	4/25/22 1:43:00 PM
--------------------------------	-----------------------	---------------------------

Font color: Text 1

Page 18: [99] Formatted	Amanda Schmidt	4/25/22 1:43:00 PM
--------------------------------	-----------------------	---------------------------

Font color: Text 1

Page 18: [100] Formatted	Amanda Schmidt	4/25/22 1:43:00 PM
---------------------------------	-----------------------	---------------------------

Font color: Text 1

Page 18: [101] Formatted	Amanda Schmidt	4/25/22 1:43:00 PM
---------------------------------	-----------------------	---------------------------

Font color: Text 1

Page 18: [102] Formatted	Amanda Schmidt	4/25/22 1:43:00 PM
---------------------------------	-----------------------	---------------------------

Font color: Text 1

Page 18: [102] Formatted	Amanda Schmidt	4/25/22 1:43:00 PM
---------------------------------	-----------------------	---------------------------

Font color: Text 1

Page 18: [103] Formatted	Amanda Schmidt	4/25/22 1:43:00 PM
---------------------------------	-----------------------	---------------------------

Font color: Text 1

Page 18: [104] Formatted	Amanda Schmidt	4/25/22 1:43:00 PM
---------------------------------	-----------------------	---------------------------

Font color: Text 1

Page 18: [105] Formatted	Amanda Schmidt	4/25/22 1:43:00 PM
---------------------------------	-----------------------	---------------------------

Font color: Text 1

Page 18: [106] Formatted	Amanda Schmidt	4/25/22 1:43:00 PM
---------------------------------	-----------------------	---------------------------

Font color: Text 1

Page 18: [106] Formatted	Amanda Schmidt	4/25/22 1:43:00 PM
---------------------------------	-----------------------	---------------------------

Font color: Text 1

Page 18: [108] Formatted	Amanda Schmidt	4/25/22 1:43:00 PM
Font color: Text 1		
Page 18: [109] Formatted	Amanda Schmidt	4/25/22 1:43:00 PM
Font color: Text 1		
Page 18: [110] Formatted	Amanda Schmidt	4/25/22 1:43:00 PM
Font color: Text 1		
Page 18: [111] Formatted	Amanda Schmidt	4/25/22 1:43:00 PM
Font color: Text 1		
Page 18: [112] Formatted	Amanda Schmidt	4/25/22 1:43:00 PM
Font color: Text 1		
Page 18: [112] Formatted	Amanda Schmidt	4/25/22 1:43:00 PM
Font color: Text 1		
Page 18: [113] Formatted	Amanda Schmidt	4/25/22 1:43:00 PM
Font color: Text 1		
Page 18: [114] Formatted	Amanda Schmidt	4/25/22 1:43:00 PM
Font color: Text 1		
Page 19: [115] Formatted	Amanda Schmidt	4/25/22 1:43:00 PM
Font color: Text 1		
Page 19: [116] Formatted	Amanda Schmidt	4/25/22 1:43:00 PM
Font color: Text 1		
Page 19: [117] Formatted	Amanda Schmidt	4/25/22 1:43:00 PM
Font color: Text 1		
Page 19: [118] Formatted	Amanda Schmidt	4/25/22 1:43:00 PM
Font color: Text 1		
Page 19: [119] Formatted	Amanda Schmidt	4/25/22 1:43:00 PM
Font color: Text 1		
Page 19: [119] Formatted	Amanda Schmidt	4/25/22 1:43:00 PM
Font color: Text 1		
Page 19: [120] Formatted	Amanda Schmidt	4/25/22 1:43:00 PM
Font color: Text 1		
Page 19: [121] Formatted	Amanda Schmidt	4/25/22 1:43:00 PM
Font color: Text 1		
Page 19: [122] Formatted	Amanda Schmidt	4/25/22 1:43:00 PM
Font color: Text 1		
Page 19: [123] Formatted	Amanda Schmidt	4/25/22 1:43:00 PM
Font color: Text 1		
Page 19: [124] Deleted	Amanda Schmidt	4/25/22 1:43:00 PM

Font color: Text 1

Page 19: [126] Formatted **Amanda Schmidt** **4/25/22 1:43:00 PM**

Font color: Text 1

Page 19: [127] Formatted **Amanda Schmidt** **4/25/22 1:43:00 PM**

Font color: Text 1

Page 19: [128] Formatted **Amanda Schmidt** **4/25/22 1:43:00 PM**

Font color: Text 1

Page 19: [129] Formatted **Amanda Schmidt** **4/25/22 1:43:00 PM**

Font color: Text 1

Page 19: [130] Formatted **Amanda Schmidt** **4/25/22 1:43:00 PM**

Font color: Text 1

Page 19: [131] Formatted **Amanda Schmidt** **4/25/22 1:43:00 PM**

Font color: Text 1

Page 19: [132] Formatted **Amanda Schmidt** **4/25/22 1:43:00 PM**

Font color: Text 1

Page 19: [133] Formatted **Amanda Schmidt** **4/25/22 1:43:00 PM**

Font color: Text 1

Page 19: [134] Formatted **Amanda Schmidt** **4/25/22 1:43:00 PM**

Font color: Text 1

Page 19: [135] Formatted **Amanda Schmidt** **4/25/22 1:43:00 PM**

Font color: Text 1

Page 19: [136] Deleted **Amanda Schmidt** **4/25/22 1:43:00 PM**

▼

Page 19: [137] Formatted **Amanda Schmidt** **4/25/22 1:43:00 PM**

Font color: Text 1

Page 19: [138] Formatted **Amanda Schmidt** **4/25/22 1:43:00 PM**

Font color: Text 1

Page 19: [138] Formatted **Amanda Schmidt** **4/25/22 1:43:00 PM**

Font color: Text 1

Page 19: [138] Formatted **Amanda Schmidt** **4/25/22 1:43:00 PM**

Font color: Text 1

Page 19: [139] Formatted **Amanda Schmidt** **4/25/22 1:43:00 PM**

Font color: Text 1

Page 19: [139] Formatted **Amanda Schmidt** **4/25/22 1:43:00 PM**

Font color: Text 1

Page 20: [140] Formatted **Amanda Schmidt** **4/25/22 1:43:00 PM**

Font color: Text 1

Page 20: [142] Formatted	Amanda Schmidt	4/25/22 1:43:00 PM
---------------------------------	-----------------------	---------------------------

Font color: Text 1

Page 20: [143] Formatted	Amanda Schmidt	4/25/22 1:43:00 PM
---------------------------------	-----------------------	---------------------------

Font color: Text 1

Page 20: [144] Deleted	Amanda Schmidt	4/25/22 1:43:00 PM
-------------------------------	-----------------------	---------------------------

Page 20: [145] Formatted	Amanda Schmidt	4/25/22 1:43:00 PM
---------------------------------	-----------------------	---------------------------

Font: 12 pt, Font color: Text 1

Page 20: [146] Formatted	Amanda Schmidt	4/25/22 1:43:00 PM
---------------------------------	-----------------------	---------------------------

Font color: Text 1

Page 20: [147] Formatted	Amanda Schmidt	4/25/22 1:43:00 PM
---------------------------------	-----------------------	---------------------------

Font color: Text 1

Page 20: [148] Formatted	Amanda Schmidt	4/25/22 1:43:00 PM
---------------------------------	-----------------------	---------------------------

Font color: Text 1

Page 20: [149] Formatted	Amanda Schmidt	4/25/22 1:43:00 PM
---------------------------------	-----------------------	---------------------------

Font color: Text 1

Page 20: [150] Formatted	Amanda Schmidt	4/25/22 1:43:00 PM
---------------------------------	-----------------------	---------------------------

Font color: Text 1

Page 20: [150] Formatted	Amanda Schmidt	4/25/22 1:43:00 PM
---------------------------------	-----------------------	---------------------------

Font color: Text 1

Page 20: [150] Formatted	Amanda Schmidt	4/25/22 1:43:00 PM
---------------------------------	-----------------------	---------------------------

Font color: Text 1

Page 20: [151] Formatted	Amanda Schmidt	4/25/22 1:43:00 PM
---------------------------------	-----------------------	---------------------------

Font color: Text 1

Page 20: [152] Formatted	Amanda Schmidt	4/25/22 1:43:00 PM
---------------------------------	-----------------------	---------------------------

Font color: Text 1

Page 20: [153] Formatted	Amanda Schmidt	4/25/22 1:43:00 PM
---------------------------------	-----------------------	---------------------------

Font color: Text 1

Page 20: [153] Formatted	Amanda Schmidt	4/25/22 1:43:00 PM
---------------------------------	-----------------------	---------------------------

Font color: Text 1

Page 20: [154] Formatted	Amanda Schmidt	4/25/22 1:43:00 PM
---------------------------------	-----------------------	---------------------------

Font color: Text 1

Page 20: [155] Formatted	Amanda Schmidt	4/25/22 1:43:00 PM
---------------------------------	-----------------------	---------------------------

Font color: Text 1

Page 20: [156] Formatted	Amanda Schmidt	4/25/22 1:43:00 PM
---------------------------------	-----------------------	---------------------------

Font color: Text 1

Page 20: [157] Formatted	Amanda Schmidt	4/25/22 1:43:00 PM
---------------------------------	-----------------------	---------------------------

Font color: Text 1

Page 20: [159] Formatted	Amanda Schmidt	4/25/22 1:43:00 PM
---------------------------------	-----------------------	---------------------------

Font color: Text 1

Page 20: [160] Formatted	Amanda Schmidt	4/25/22 1:43:00 PM
---------------------------------	-----------------------	---------------------------

Font color: Text 1

Page 20: [161] Formatted	Amanda Schmidt	4/25/22 1:43:00 PM
---------------------------------	-----------------------	---------------------------

Font color: Text 1

Page 20: [162] Formatted	Amanda Schmidt	4/25/22 1:43:00 PM
---------------------------------	-----------------------	---------------------------

Font color: Text 1

Page 28: [163] Deleted	Amanda Schmidt	4/25/22 1:43:00 PM
-------------------------------	-----------------------	---------------------------

▼

Page 29: [164] Formatted	Amanda Schmidt	4/25/22 1:43:00 PM
---------------------------------	-----------------------	---------------------------

Font: 12 pt, Not Bold

Page 29: [164] Formatted	Amanda Schmidt	4/25/22 1:43:00 PM
---------------------------------	-----------------------	---------------------------

Font: 12 pt, Not Bold